

fractalRegression: An R package for multiscale regression and fractal analyses

Aaron D. Likens¹ & Travis J. Wiltshire²

¹ Department of Biomechanics, University of Nebraska at Omaha

² Department of Cognitive Science & Artificial Intelligence, Tilburg University

Author Note

The authors made the following contributions. Aaron D. Likens: Conceptualization, Software, Writing - Original Draft Preparation, Writing - Review & Editing; Travis J. Wiltshire: Writing - Original Draft Preparation, Writing - Review & Editing, Software.

Correspondence concerning this article should be addressed to Aaron D. Likens, Division of Biomechanics and Research Development, Department of Biomechanics, and Center for Research in Human Movement Variability, University of Nebraska at Omaha, 6160 University Dr S, Omaha, 68182, NE, USA.. E-mail: alikens@unomaha.edu

Abstract

Time series data from scientific fields as diverse as astrophysics, economics, human movement science, and neuroscience all exhibit fractal properties. That is, these time series often exhibit self-similarity and long-range correlations. This **fractalRegression** package implements a number of univariate and bivariate time series tools appropriate for analyzing noisy data exhibiting these properties. These methods, especially the bivariate tools (Kristoufek, 2015a; Likens, Amazeen, West, & Gibbons, 2019a) have yet to be implemented in an open source and complete package for the R Statistical Software environment. As both practitioners and developers of these methods, we expect these tools will be of interest to a wide audience of scientists who use R, especially those from fields such as the human movement, cognitive, and other behavioral sciences. The algorithms have been developed in C++ using the popular Rcpp (Eddelbuettel & Francois, 2011) and RcppArmadillo (Eddelbuettel & Sanderson, 2014) packages. The result is a collection of efficient functions that perform well even on long time series (e.g., $\geq 10,000$ data points). In this work, we introduce the package, each of the functions, and give examples of their use as well as issues to consider to correctly use these methods.

Keywords: long range correlation, fractal, multiscale, dynamical systems

Word count: 6,888

fractalRegression: An R package for multiscale regression and fractal analyses

Introduction

Over time, many signals from living and complex systems exhibit systematic regularities and dependencies across spatial and temporal scales (Kello et al., 2010). These regularities often follow a power-law (i.e., self-similarity across scales) that are estimated using fractal analyses. Fractal analysis, in its many forms, has become an important framework in virtually every area of science, often serving as an indicator of system health (Goldberger et al., 2002), adaptability (Bak, Tang, & Wiesenfeld, 1987), control (Likens, Fine, Amazeen, & Amazeen, 2015), cognitive function (Euler, Wiltshire, Niermeyer, & Butner, 2016), and multi-scale interactions (Kelty-Stephen, 2017).

In particular, various methods related to Detrended Fluctuation Analysis (DFA) (Peng et al., 1994) have rose to prominence due to their relative ease of understanding and broad applicability to stationary and non-stationary time series, alike. More specifically, in areas of the social and cognitive sciences, DFA, or variants of DFA, have been used to study, for example, reaction times (Van Orden, Holden, & Turvey, 2003), eye gaze (Stephen, Boncoddo, Magnuson, & Dixon, 2009), gait (Delignières & Torre, 2009; Hausdorff et al., 1996), limb movements (Delignières, Torre, & Lemoine, 2008), heart rate (Goldberger et al., 2002), and neurophysiological oscillations (Euler et al., 2016; Hardstone et al., 2012; Schaworonkow & Voytek, 2021). Beyond an individual level, the methods have been used to study human-machine system interaction (Likens et al., 2015), tool use (Favela, 2020; Kelty-Stephen, Stirling, & Lipsitz, 2016), and interpersonal coordination in a variety of modalities (Davis, Brooks, & Dixon, 2016; Delignières, Almurad, Roume, & Marmelat, 2016).

Thus, there is a broad scientific appeal for these fractal-based analyses. While, the basic DFA algorithm has been implemented in numerous packages and software programs, more advanced methods such as Multifractal Detrended Fluctuation Analysis (MFDFA)

(Kantelhardt et al., 2002), Detrended Cross Correlation Analysis (DCCA) (Podobnik & Stanley, 2008; Zebende, 2011), and, in particular, fractal regression techniques such as Multiscale Regression Analysis (MRA) (Kristoufek, 2015a; Likens et al., 2019a) have not yet been implemented in a comprehensive software package. A key aspect of this effort is to draw more attention and make more available these *fractal regression* techniques. In particular, we find these methods widely promising because they allow for uncovering “the time scales most relevant to relationships between a system’s components” (p. 2) within a predictive framework (Likens et al., 2019a).

Thus, there is a clear need for a package that incorporates this functionality in order to advance theoretical research focused on understanding the time varying properties of natural phenomena and applied research that uses those insights in important and diverse areas such as healthcare (Cavanaugh, Kelty-Stephen, & Stergiou, 2017) and education (Snow, Likens, Allen, & McNamara, 2016). In this work, we provide an overview of our **fractalRegression** package, provide simulated and empirical examples of its functions, and provide practical advice on the successful application of these methods.

Package Overview

Our **fractalRegression** package for R (Team, 2018) is built for speed, based on a C++ architecture and includes a variety of uni- and bivariate fractal methods as well as functions for simulating data with known fractional properties (e.g., scaling, dependence, etc.), and surrogate testing. Some foundational efforts in fractal analyses, which partially overlap with the functionality of this package, have been implemented elsewhere. For example, a number of univariate fractal and multifractal analyses have been implemented in the ‘fracLab’ library for MATLAB (Legrand & Véhel, 2003) and other toolboxes that are mainly targeted at multifractal analysis (Ihlen, 2012; Ihlen & Vereijken, 2010). In terms of open access packages, there are other packages that implement some, but not all of the same functions such as the **fathon** package (Bianchi, 2020) that has been

implemented in Python as well as the R packages: `fractal` [defunct], `nonlinearTseries` (Garcia, 2020), and `MF DFA` (Laib, Golay, Telesca, & Kanevski, 2018). However, none of the above packages incorporate univariate monofractal and multifractal DFA with bivariate DCCA and MRA and some are only written in base R code, which can be less efficient for long time series. Our `fractalRegression` package is unique in this combination of analyses and efficiency (particularly for long time series). For instance, we are not aware of any other packages that feature MRA. In addition, we expect that featuring simulation methods as well as surrogate testing strongly bolsters the accessibility of these methods for the social and cognitive science community in particular, but also science, more generally. An overview of the core functions included in the package, the general objective of that function, and the output are shown below in Table 1. Note that there are some additional helper and plotting functions included as well. The additional details are included in the sections corresponding to those methods, in the package documentation, and in the original sources for the methods.

Table 1.

Overview of core package functions, objectives, and output

Methodological Details and Examples

In order to demonstrate the methods within the `fractalRegression` package, we group this into univariate (DFA, MF DFA) and bivariate methods (DCCA, MRA). For each method, we 1) highlight the key question(s) that can be answered with that method, 2) briefly describe the algorithm with references to additional details (see also Appendix 1 for fundamental equations), 3) describe some key considerations for appropriately applying the algorithm, and demonstrate the use of the functions on a 4) simulated and 5) empirical example. Note that all code, data, and text are part of a reproducible manuscript that are accessible at the following link:

https://github.com/travisjwiltshire/fractal_regression_manuscript.

Univariate Methods

Detrended Fluctuation Analysis. A key question that can be answered by Detrended Fluctuation Analysis (DFA) (Peng et al., 1994) is: *what is the magnitude and direction of long range correlation in a single time series?* While DFA has been described extensively (Kantelhardt, Koscielny-Bunde, Rego, Havlin, & Bunde, 2001) and visualized nicely elsewhere (Kelty-Stephen et al., 2016), we provide a brief summary here. DFA entails splitting a time series into several small bins (e.g., 16). In each bin, a least squares regression is fit and subtracted within each window. Residuals are squared and averaged within each window. Then, the square root is taken of the average squared residual across all windows of a given size. This process repeats for larger window sizes, growing by, say a power of 2, up to $N/4$, where N is the length of the series. In a final step, the logarithm of those scaled root mean squared residuals (i.e., fluctuations) is regressed on the logarithm of window sizes. The slope of this line is termed α and it provides a measure of the long range correlation. α is commonly used as an estimator of the Hurst exponent (H), where $\alpha < 1$ is anti-correlated, $\alpha = 0.5$ is uncorrelated, white noise, $\alpha > 0.5$ is temporally correlated, $\alpha = 1$ is long-range correlated, 1/f-noise, pink noise, $\alpha > 1$ is non-stationary where the special case $\alpha = 1.5$ is fractional Brownian noise. More generally, $1 < \alpha < 2$ are referred to as fractional Brownian motion.

DFA Examples. To demonstrate the use of `dfa()` we simulate three time series using the `fgn_sim()` function. This is a simple function based on the former `fARMA` R package [defunct]. It requires the number of observations `n`, and the Hurst exponent `H`. In particular, we simulate white noise, pink noise, and anti-correlated fractional Gaussian noise using the code below.

```
white.noise <- fgn_sim(n = 5000, H = 0.5)

pink.noise <- fgn_sim(n = 5000, H = 0.9)

anti.corr.noise <- fgn_sim(n = 5000, H = 0.25)
```

133 Then, we run DFA on those simulated series using the example code below. Note
134 that this example uses linear detrending with minimum scale of 16, a maximum scale that
135 is at most 1/4 the time series length, and scale factor (`scale_ratio`) of 2, which is evenly
136 spaced in the logarithmic domain (see General Discussion for more details and
137 considerations for these parameter choices).

```
scales <- logscale(scale_min = 16, scale_max = 1024, scale_ratio = 2)

dfa.white <- dfa(x = white.noise, order = 1, verbose = 1,
scales=scales, scale_ratio = 2)

dfa.pink <- dfa(x = pink.noise, order = 1, verbose = 1,
scales = scales, scale_ratio = 2)

dfa.anti.corr <- dfa(x = anti.corr.noise, order = 1, verbose = 1,
scales = scales, scale_ratio = 2)
```

138 In terms of output from the above examples, for white noise, we observed that $\alpha =$
139 0.50, for pink noise we observed that $\alpha = 0.82$, and since we simulated anti-correlated noise
140 with $H = 0.25$, we observed a close estimate of $\alpha = 0.24$. In terms of the objects saved
141 from the `dfa()` function, one commonly inspects the `log(scales)-log(fluctuation)` plots,
142 which we generate from our package using the `dfa.plot()` function. Given the estimates

above, we see in Figure 1 that the slopes for white noise, pink noise, and anti-correlated noise conform to our expectations. These slope estimates (and R^2) are provided in the equation listed above each respective line.

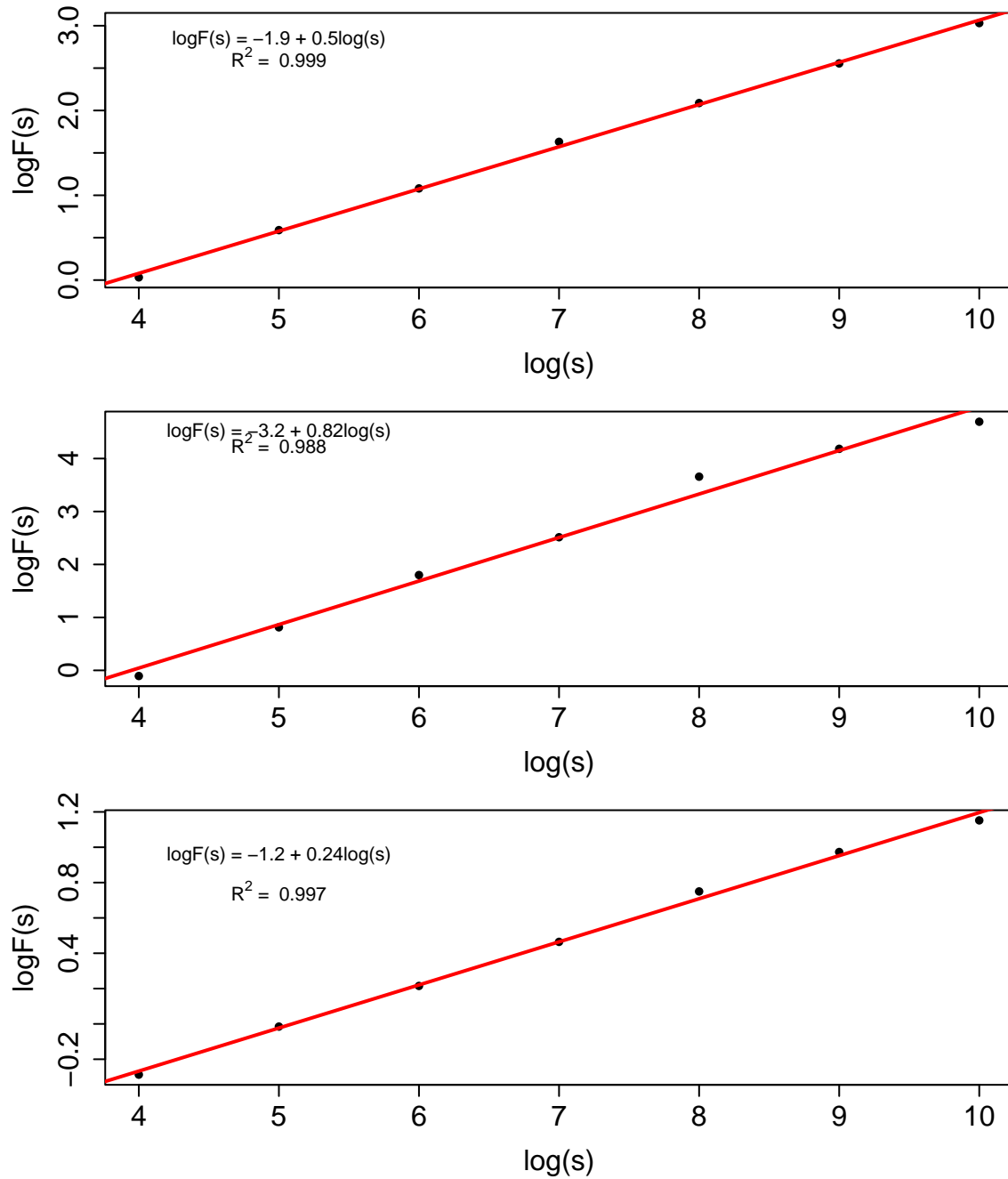


Figure 1. Log scale-Log fluctuation plots for white noise (top), pink noise (middle), and anti-correlated noise (bottom)

For an empirical example, we apply the `dfa()` function to the Human Balance Dataset (Santos & Duarte, 2016). This publicly available dataset includes signals from a force platform that measures the center of pressure in the x and y dimensions for 87 young adults (we exclude the older adults from our analyses for simplicity). Trials lasted 60s. See original paper for additional details on data processing (Santos & Duarte, 2016). For the empirical examples, we use two different time series featuring a participant standing on a firm (rigid) surface with eyes open and a foam (unstable) surface with eyes open. We chose this dataset because postural sway data are known to exhibit interesting fractal dynamics (Collins & De Luca, 1993; Delignières, Torre, & Bernard, 2011a; Delignières, Torre, & Bernard, 2011b) and we can systematically evaluate the data for all of the univariate and bivariate analyses included in the package.

For center of pressure (COP) data, we take the first order differences of each series using the `diff()` function as a rough approximation of COP velocity. For the univariate analyses, we focus on analyses of the COP data in the x dimension. Then, we define the appropriate scales for the analyses using the same methods shown above, except we use a `scale ratio = 1.1` for a higher density of points. Figure 2 shows the results of these analyses.

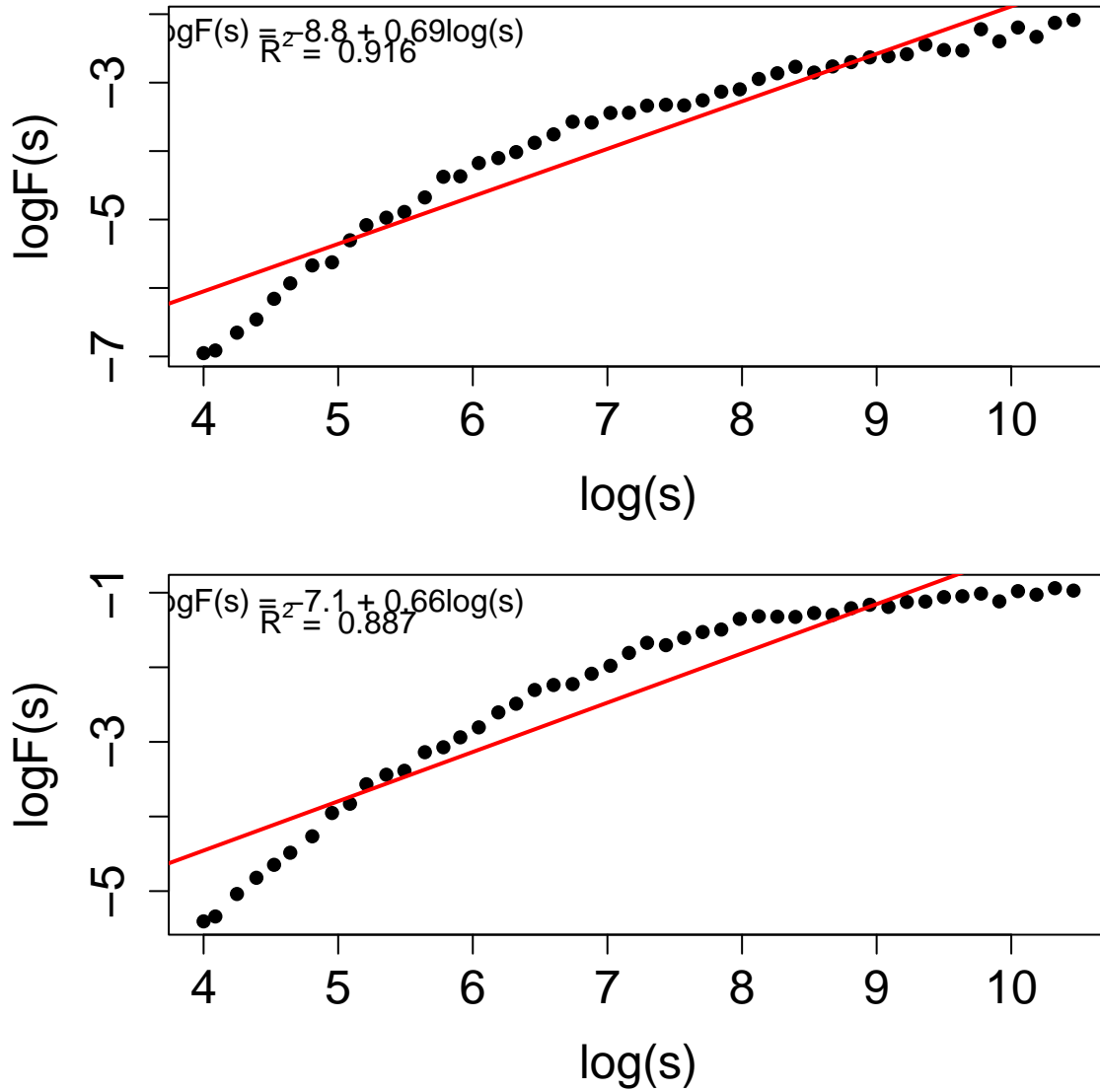


Figure 2. Log scale-Log fluctuation plots for empirical differenced COPx time series for rigid/firm (top) and unstable/foam (bottom) surfaces.

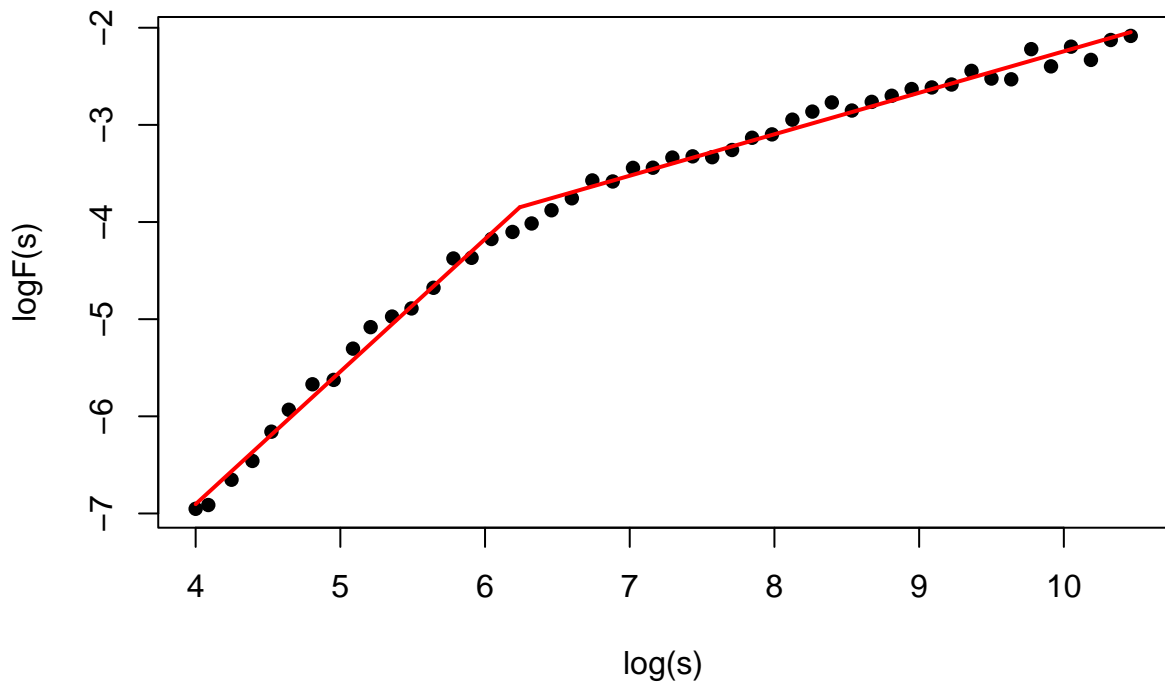
Importantly, regarding the question one can ask using DFA, we observe from Figure 2, that long range correlations are positive and approximately 0.69 - 0.66. However, from visual inspection of these plots we observe that two slopes might fit better than one for these time series; a phenomenon known as crossover points (Collins & De Luca, 1993; Ge & Leung, 2013). One common approach when such crossover points exist is to recognize that the signal might be best characterized by two scaling regions, before and after an inflection

175 point. We provide an example of how to check for where the break point is below using
 176 piece-wise regression .

```
# requires the segmented R package
```

```
dfa.mod <- lm(log_rms ~ log_scales, data = open_firm_copx_diff_dfa)
```

```
seg <- segmented(dfa.mod, seg.Z = ~log_scales)
```



177

178 **Figure 3.** *Log scale-Log fluctuation plots for empirical differenced COPx time series*
 179 *for rigid/firm surfaces with lines plotted for piece-wise regression slopes*

180 In the example above, we observe a crossover point at around the scale size of log 6.
 181 And, from the results in Table 2 below, we observe that there are two distinct scaling
 182 relationships corresponding to $\alpha = 1.36$ and $\alpha = 0.43$, respectively. This is a well known

result in the postural control literature such that short time scales exhibit a persistent temporal correlation and that longer time scales exhibit an anti-persistent correlation. More substantively, short time scale dynamics correspond to periods of exploratory sway, whereas longer time scales correspond to corrective movements that prevent exceeding the base of support and falling (Collins & De Luca, 1993; Delignières et al., 2011a; Delignières et al., 2011b).

Table 2. *Results from piece-wise regression analysis*

Multifractal Detrended Fluctuation Analysis. Multifractal Detrended Fluctuation Analysis (MFDFA; Kantelhardt et al. (2002)) is an extension of DFA by generalizing the fluctuation function to a range of exponents of the q th order. The key question that can be answered by MFDFA is: *how does the magnitude and direction of long range correlation change over time within a single time series?* Like DFA, MFDFA entails splitting a time series into several small bins (e.g., 16). In each bin, least squares regression is fit and subtracted within each window. However, the residuals are raised to a range of exponents q and averaged within each window. So when $q = 2$, MFDFA reduces to ordinary DFA. When $q > 2$, relatively larger residuals are emphasized and when $q < 2$, relatively smaller residuals are emphasized. The rest of the DFA algorithm is performed for each window and windows size for all values of q . We refer the reader to the work of Kelty-Stephens and colleagues' (Kelty-Stephen et al., 2016) Figure 3 for a visualization of the algorithm, Appendix 1 of this paper for fundamental equations, and Kantelhardt and colleagues' work (Kantelhardt et al., 2002) for additional mathematical description.

MFDFA Examples. To demonstrate the use of `mfdfa()`, we work with data included in our package (`fractaldata`), that was originally provided by Ihlen (2012). It includes a white noise time series, a monofractal time series, and a multifractal time series. These data are shown below in Figure 4.

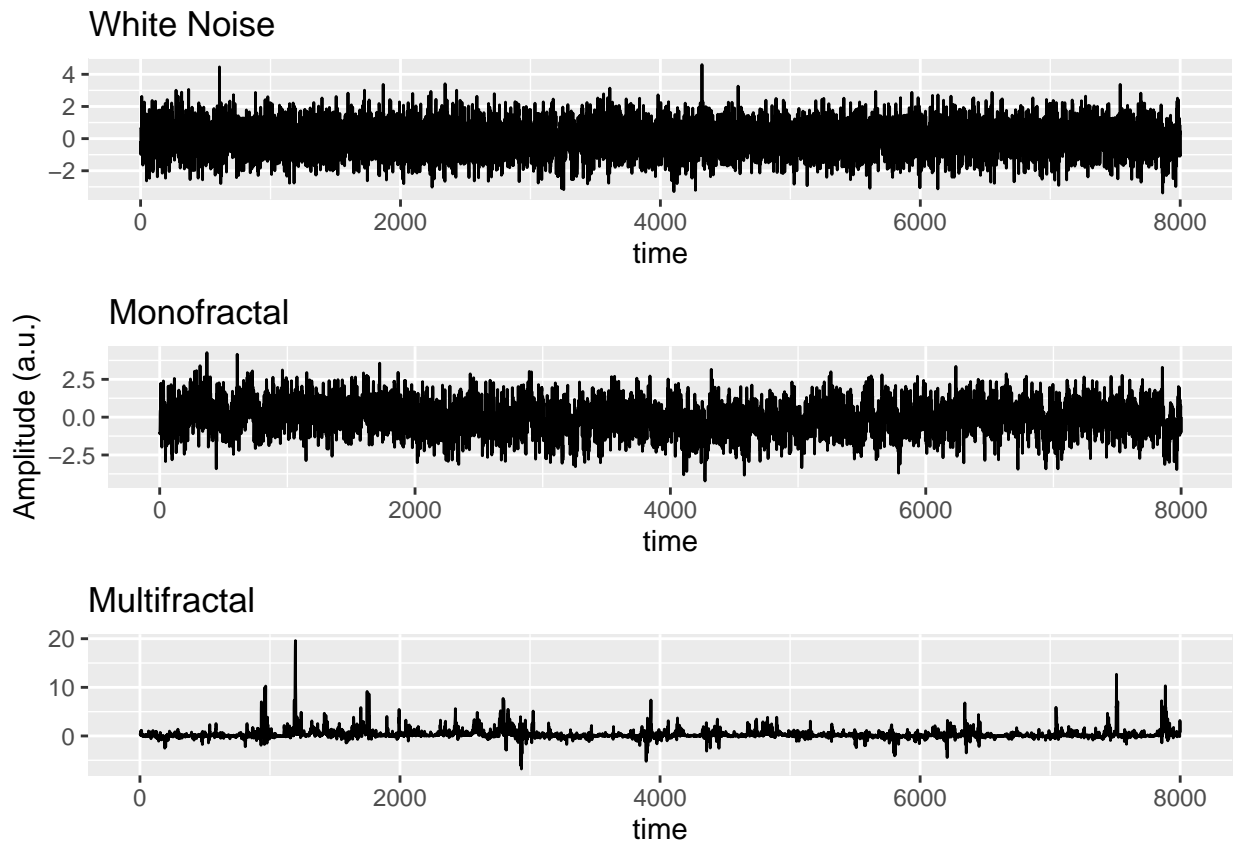


Figure 4. Time series from Ihlen (2012) corresponding to white noise, monofractal, and multifractal series

Performing MFDFA is straight forward with the `mfdfa()` function. As shown in the example below, one enters the time series `x` to perform the analysis on, the range of `q` order exponents to use, the `order` of polynomial detrending, and the `scales` for the analysis. In this case, we define our `scales` by choosing logarithmically spaced scales and we select values of `q` from -5 to 5. Note here that the scale factor need not be a power of two but should be evenly spaced in the logarithmic domain by, for example, using different logarithm bases. We provide the `logscale()` function to facilitate scale construction.

```
scales <- logscale(scale_min = 16, scale_max = 1024, scale_ratio = 1.1)

white.mf.dfa.out <- mfdfa(x = fractaldata$whitenoise, q = c(-5:5),
```

```

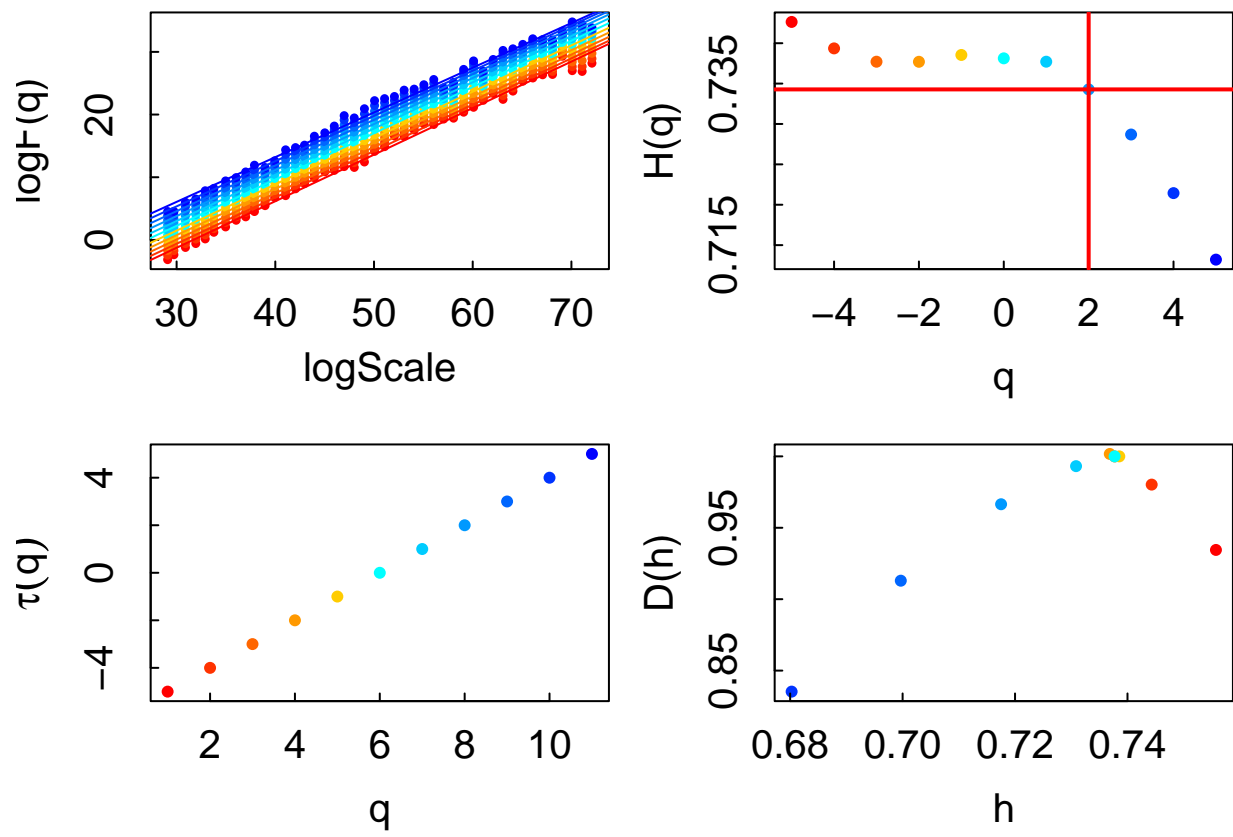
order = 1, scales=scales, scale_ratio=1.1)

mono.mf.dfa.out <- mfdfa(x = fractaldata$monofractal, q = c(-5:5),
order = 1, scales=scales, scale_ratio=1.1)

multi.mf.dfa.out <- mfdfa(x = fractaldata$multifractal, q = c(-5:5),
order = 1, scales=scales, scale_ratio=1.1)

```

218 A common way to understand if there is evidence of multifractality is to examine a
 219 plot showing the slopes of the `log_fq` at the `log_scale` values. If all the lines have the
 220 same slope, that provides evidence of monofractality. If there are distinct slopes, then there
 221 is evidence of multifractality. It's also important to check here that the slopes of
 222 `log_scale` and `log_fq` are approximately linear, thus implying that they are scale
 223 invariant. If not, then it could be the case that a higher order polynomial detrending is
 224 appropriate (see Kantelhardt et al., 2001). Figure 5, in the top left quadrants, shows what
 225 we would expect for a monofractal and multifractal signal. In other words, the monofractal
 226 signal shows a consistent slope, whereas the multifractal signal shows variability in the
 227 slopes. Importantly, Figure 5, using our `mfdfa.plot()` function, shows various aspects of
 228 `mfdfa` for each value of `q` (each with its own color) and includes panels that show the
 229 $\log(\text{scale})$ - $\log(\text{Fluctuation})$ plots like in the DFA plots (top left), the slopes of those lines as
 230 the q -order Hurst exponents $H(q)$ for each value of q (top right), the mass exponents
 231 $(\tau(q))$ for each value of q (bottom left), and the multifractal spectrum showing q -order
 232 singularity values (h) for their dimension ($D(h)$) for each value of q (bottom right). See
 233 Ihlen (2012) for additional details of these metrics.



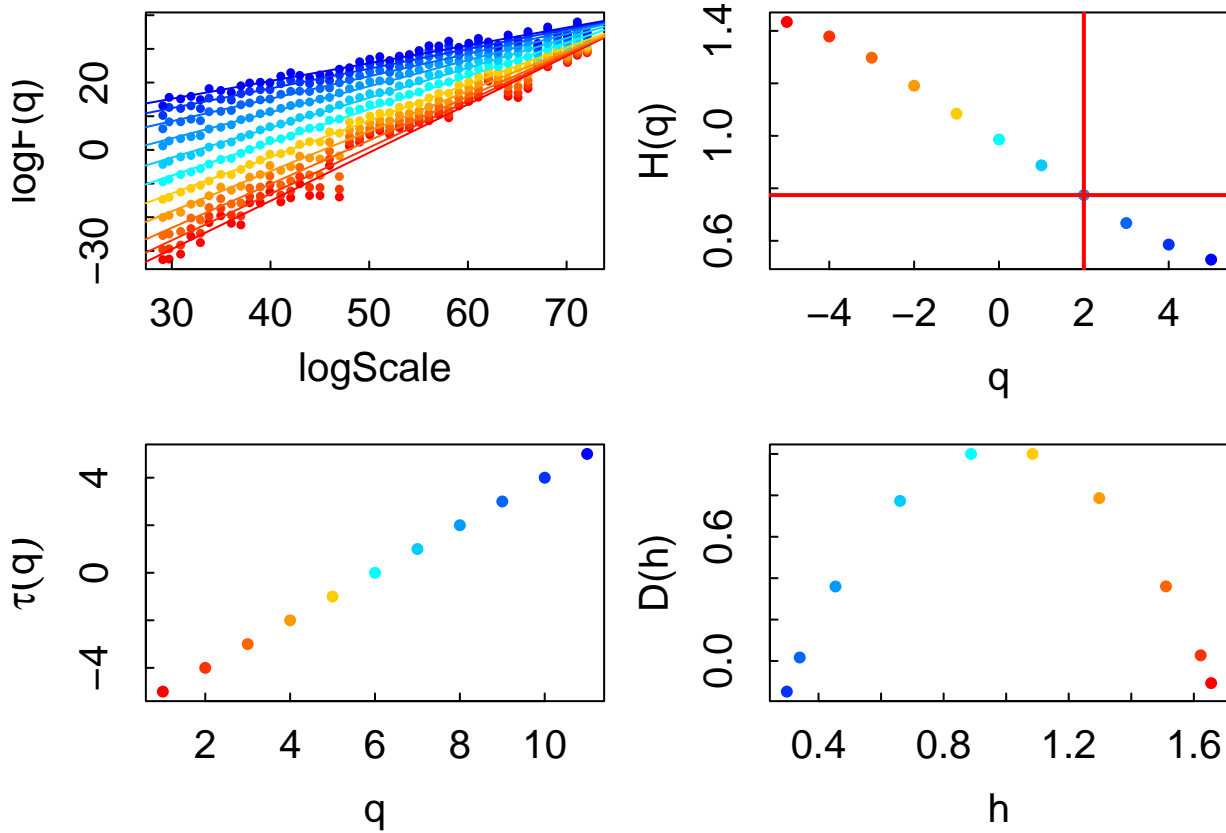
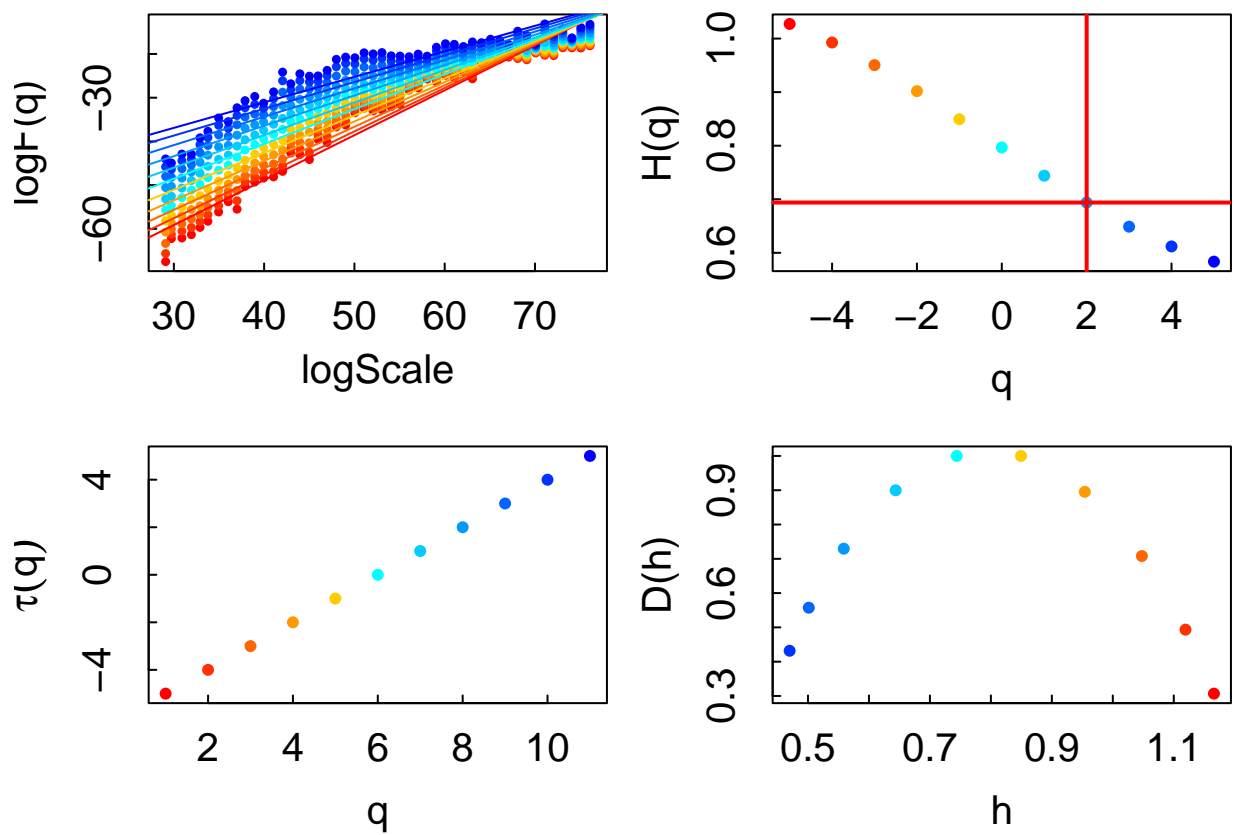


Figure 5. *mfdfa.plots* for mono-(top) and multifractal series (bottom).

A common metric for comparing multifractal spectra is to calculate the width (W) as $h_{max} - h_{min}$. Let's do this to compare the monofractal and multifractal time series. We observe in this case that for the monofractal signal $W_{mono} = 0.08$ and $W_{multi} = 1.36$. If we compare the spectra for the mono- and multifractal signals above (bottom right of both plots), we observe this clear difference in the widths of the multifractal spectra for the signals.

For our empirical analysis, we again turn to the postural data. We set our parameters appropriate for the data and run `mfdfa()` on the differenced COPx data for the firm and foam surfaces. Figure 6 shows the plots for these analyses. In particular, we observe for both surfaces that the q -order Hurst exponents range from 0.57 - 1.03, all suggesting positive long-range correlations with a weakening of the strength at larger values of q (i.e.,

248 trending towards white noise). The multifractal spectrum widths of the two surfaces were
 249 also similar, $W_{foam} = 0.69$ and $W_{firm} = 0.70$.



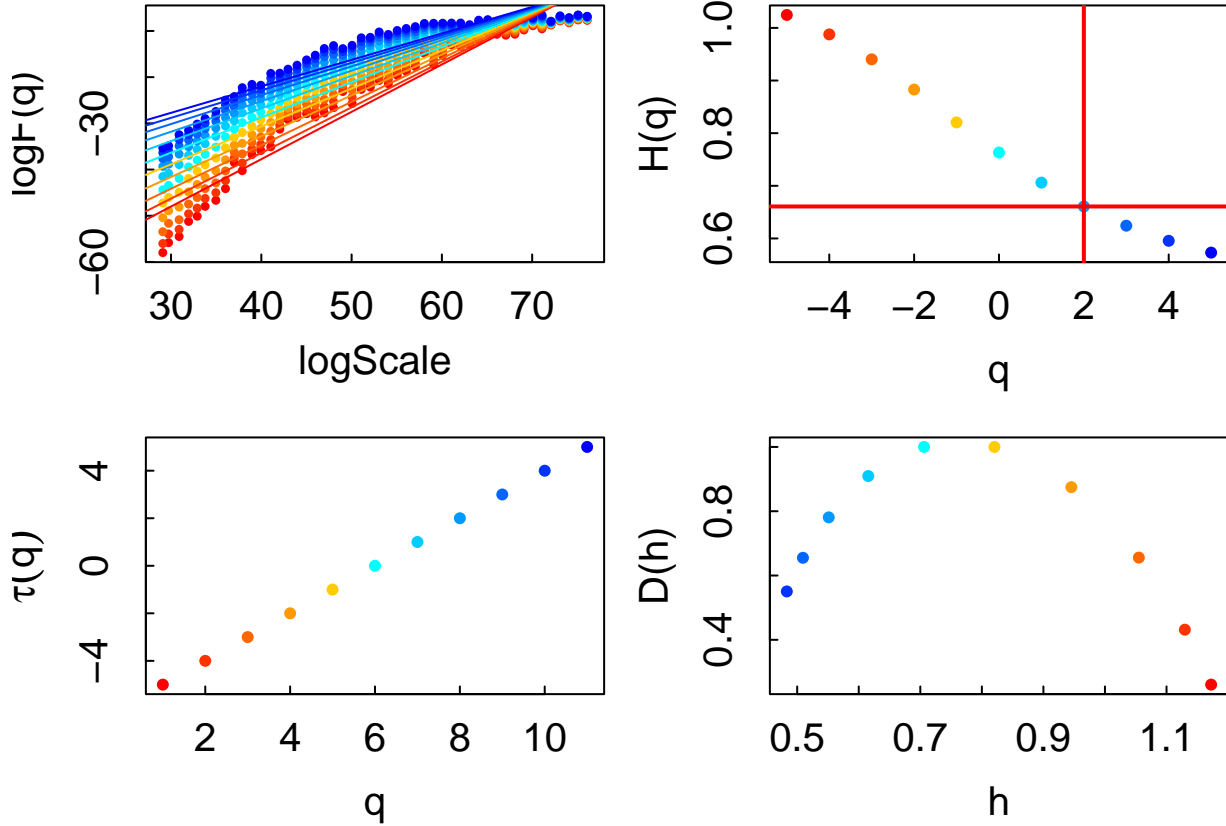


Figure 6. *mfdfa.plots* for the firm (top) and foam surfaces (bottom).

Bivariate Methods

Detrended Cross-Correlation Analysis.

Detrended Cross-Correlation Analysis (DCCA (Podobnik & Stanley, 2008; Zebende, 2011) is a bivariate extension of the DFA algorithm generalizing it to a correlational case between two time series that may be non-stationary. The key questions that can be asked with it are: a) *How does the correlation between two time series change as a function of scale?* and b) *What is/are the dominant (time) scale(s) of coordination?* Such decisions are based on a predetermined threshold such as a conventional statistical significance as we demonstrate below. Researchers may also select other criteria appropriate for their research area. The DCCA algorithm is a direct generalization of the DFA algorithm but applied to two concomitantly measured time series, say x and y . As in DFA, time series are split into multiple bins and

detrended using least squares regression. Separate regressions are performed for x and y . Within each bin, three quantities are estimated, the average squared residual of x , the average squared residual of y , and the average cross product (i.e., the covariance) between the residuals for x and the residuals for y . Each of those quantities is averaged across all bins of a given size. After taking the squared residual for x and y , we obtain scale-wise equivalents of covariance $F_{xy}(s)$ and standard deviations for x $F_x(s)$ and y $F_y(s)$. The use of F to designate these quantities derives from originating literature (Kristoufek, 2015b; Likens, Amazeen, West, & Gibbons, 2019b). Thus, the scale-wise regression coefficient, the estimand of DCCA, is the following quotient:

$$\rho(s) = \frac{F_{xy}(s)}{F_x(s)F_y(s)}$$

Simplified, in DFA, the key metric is α , but in DCCA, one estimates the scale-specific, detrended cross-correlation coefficient $\rho(s)$ for the pair of time series.

DCCA Examples. To demonstrate the use of `dcca()`, we used the `mc_arfima()` function from our package to simulate two time series with known properties. Specifically, we use the multicorrelated ARFIMA examples from Kristoufek’s work (Kristoufek, 2013). In this case, we use the parameters from Kristoufek (2013) for Model 1 (p. 6,487), that generates two time series of length 10,000 that exhibit long range correlations (LRC) as well as long range cross-correlations (LRCC). The code for simulating these two time series is shown below. Additionally, Figure 7, shown below, visualizes a subset of these time series.

```
set.seed(987345757)

sim1 <- mc_ARFIMA(process="Mixed_ARFIMA_ARFIMA", alpha = 0.2,
  beta = 1, gamma = 1, delta = 0.2, n = 10000, d1 = 0.4, d2 = 0.3,
  d3 = 0.3, d4=0.4, rho=0.9)
```

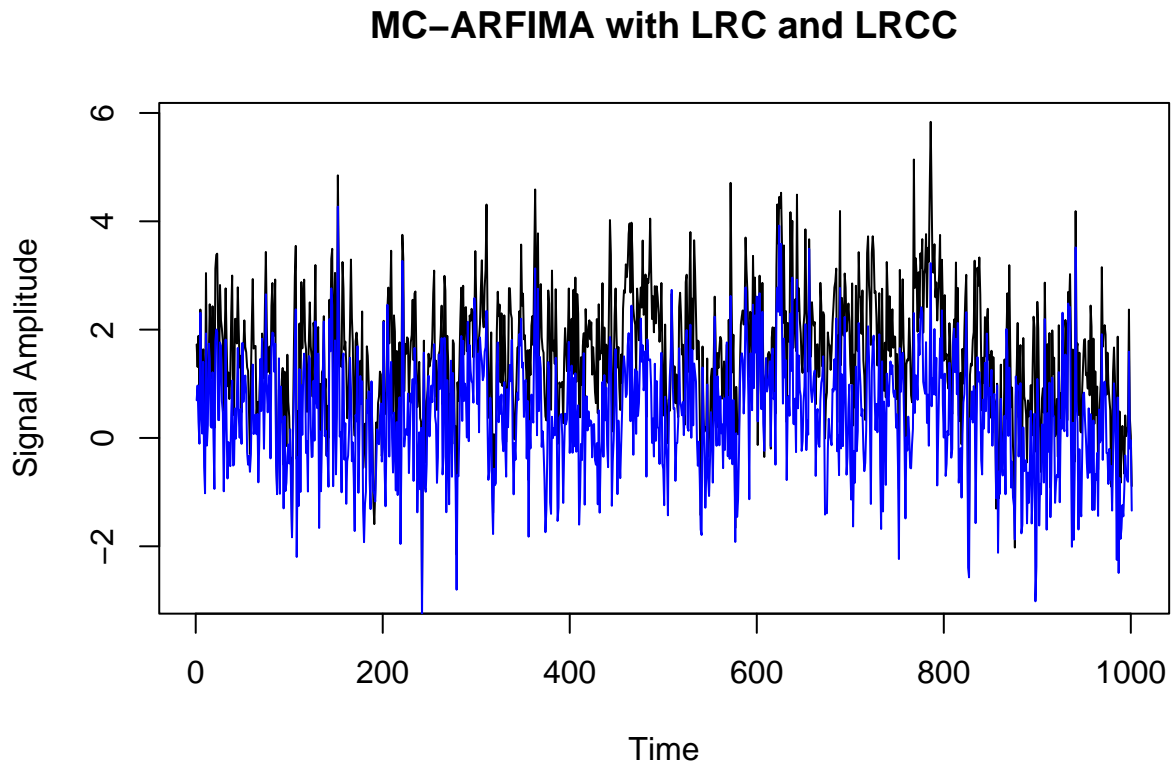


Figure 7. *Subset of two time series exhibiting long range correlation and long range cross-correlation.*

As can be seen in Figure 7, the simulated time series, although quite noisy, appear to covary over time with similar trends. To perform the `dcca()` on these time series, we use the code below, where we first define the `scales` using the `logscale()` function described earlier along with the `dcca()` function itself.

```
scales <- logscale(scale_min = 10, scale_max = 1000, scale_ratio = 1.1)

dcca.out.arfima <- dcca(sim1[,1], sim1[,2], order = 1, scales = scales)
```

Next, we visualize the output of DCCA in Figure 8. We observe that, as expected, the correlation between the MC-ARFIMA processes are consistently high (all ρ 's $> .8$) and continue to be high at increasing time scales.

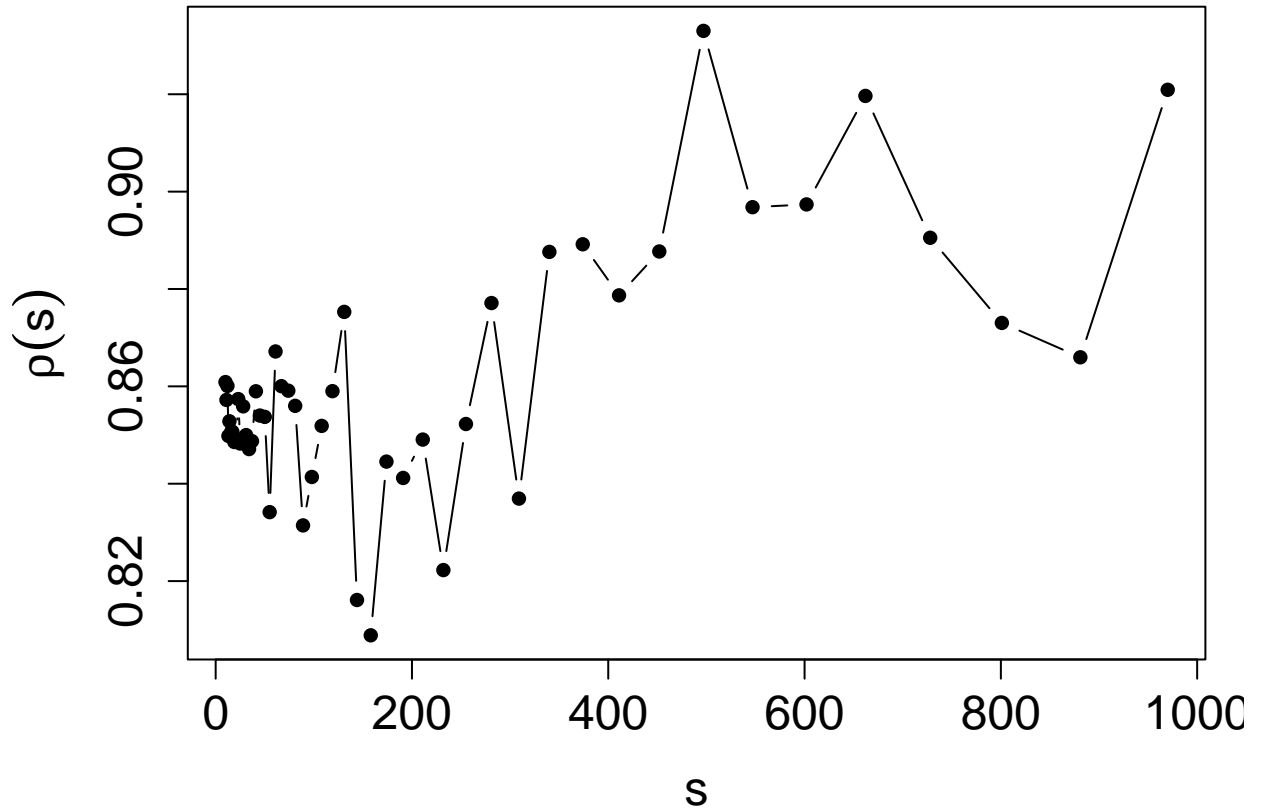


Figure 8. *DCCA output for long range correlation and long range cross-correlation.*

Figure 8 is difficult to interpret on its own. To address this, we demonstrate an additional plot and analysis feature of `dcca()` by modifying the above code as shown below `ci = TRUE`. Loess smoothing can also be applied to both $\rho(s)$ and its confidence intervals using `loess.rho = TRUE` and `loess.ci = TRUE`. Those latter options are useful for reducing the impact of increasing variance on estimates of $\rho(s)$ at large scales (Likens et al., 2019b). Note though that a much larger set of calculations takes place and may take several seconds up to several minutes (for long time series) to complete. This method is shown in Figure 9. Importantly, it shows us that there is evidence of long range cross-correlations as there $\rho(s)$ for all scales are outside of the surrogate confidence interval.

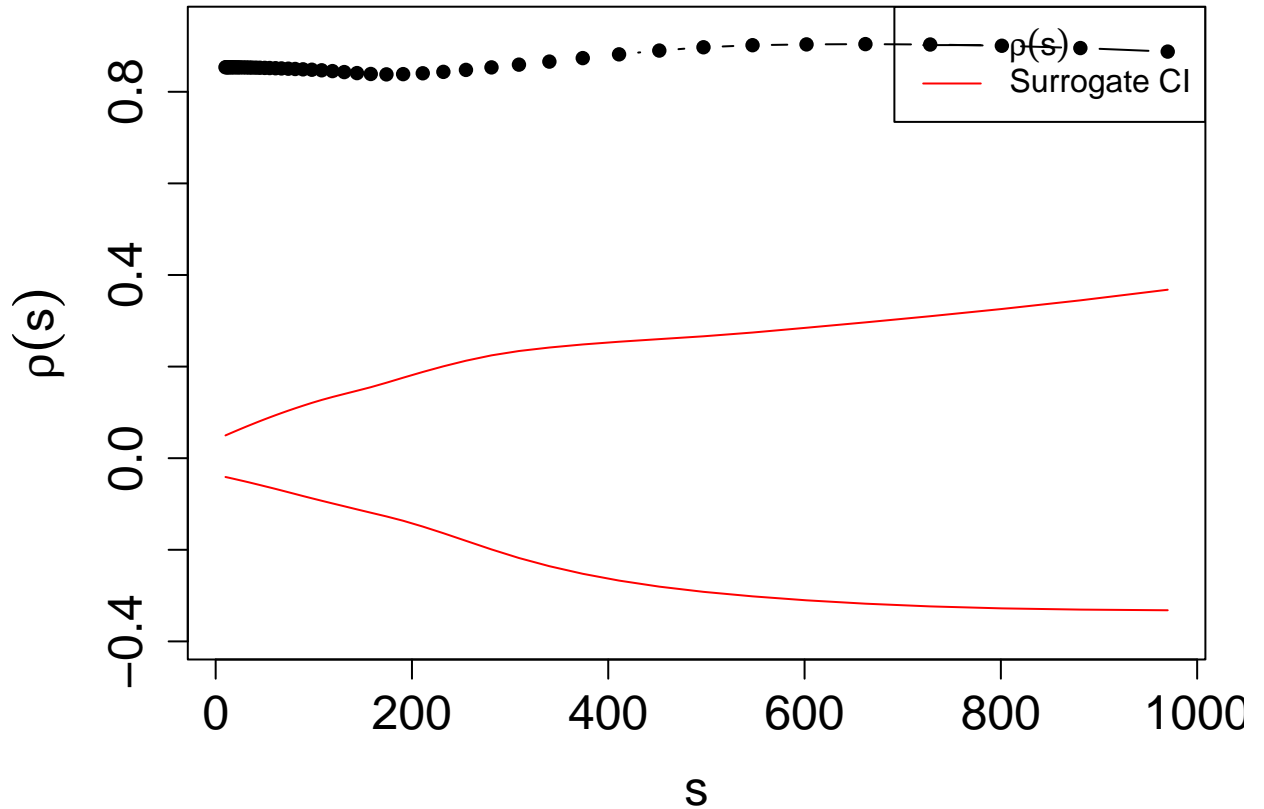


Figure 9. *DCCA output for long range correlation and long range cross-correlation with Loess smoothing on estimates and a surrogate confidence interval.*

As a point of comparison, we can generate a time series in contrast with that example that exhibit processes with LRC and short-range cross-correlation (SRCC) using the code below. In contrast to the previous DCCA analysis, Figure 10 shows a signal that begins with a high cross-correlation (ρ 's $\approx .6$), but that begins to deviate and trend substantially lower at increasing scale sizes with ρ entering the confidence interval containing 0. In fact, based on the plotted confidence intervals, the correlation between the two series becomes non-significant from a conventional standpoint.

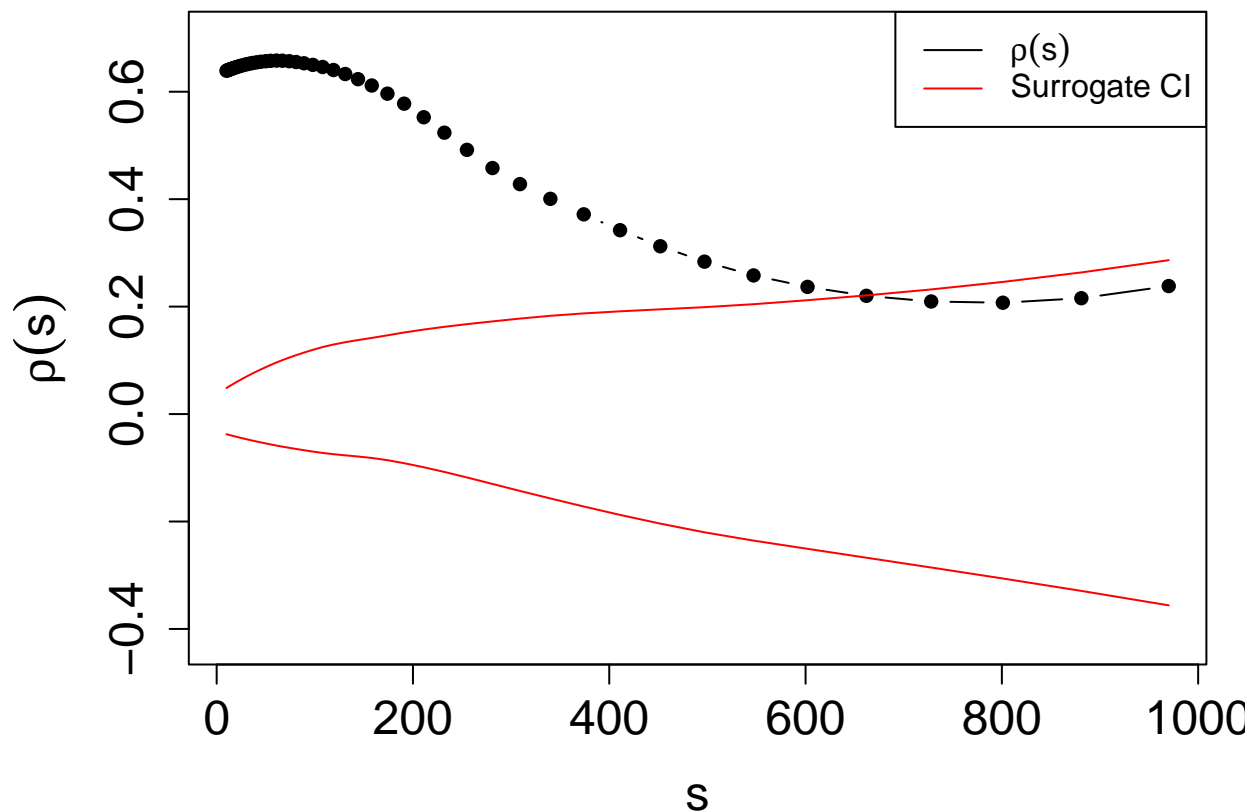
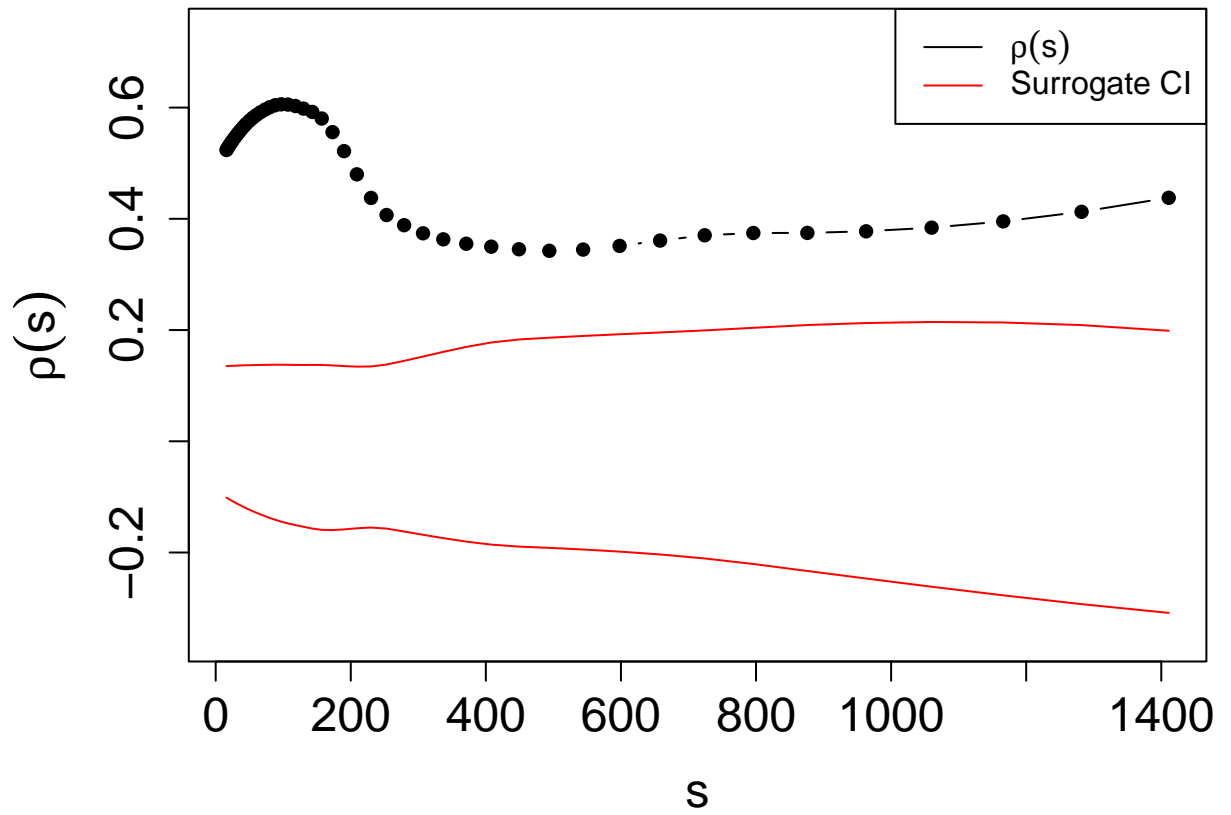


Figure 10. *DCCA output for long range correlation and short range cross-correlation including smoothing and a surrogate confidence interval.*

Turning next to the empirical balance data, we apply DCCA to the differenced COPx and COPy data for the firm and foam platforms. We again set appropriate values for scales and apply the `dcca()` function to the pair of time series.



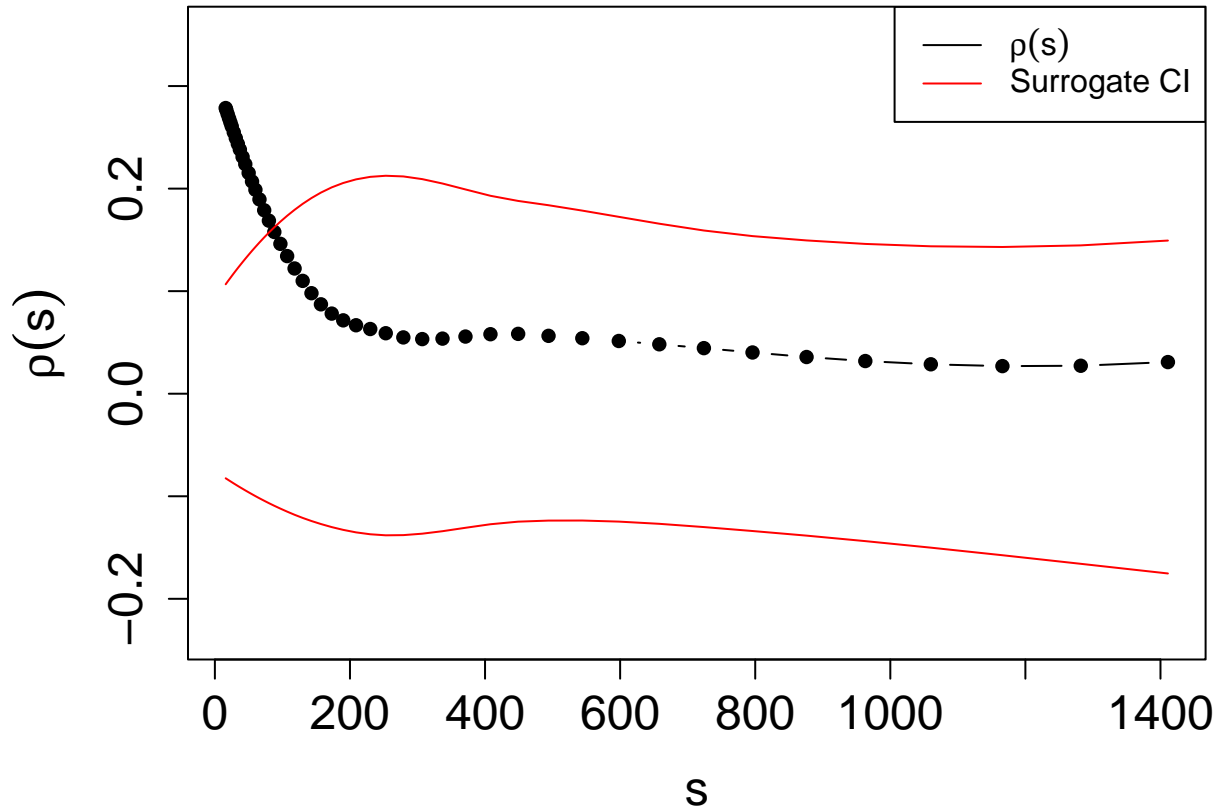


Figure 11. *DCCA output for empirical COPx and COPy balance data for the eyes open while standing on the firm surface (top) and foam surface (bottom)*

In examining the output from these analyses, Figure 11 shows a clear difference between the two conditions. First, in the firm platform example, the $\rho(s)$ values are much greater than in the foam condition with the max $\rho(s) = 0.73$ compared to 0.35 for the foam condition. Second, we observe for the foam example, that the time scale of maximum correlation is 73, which is a larger time scale when compared to the foam example, which had a maximum correlation at scale 16. Third, the pattern of change in correlation across scales is slightly different. The firm example is higher overall; it starts relatively low at very small time scales before a rapid increase and then steady decrease before stabilizing at increasingly larger scales. By contrast, the foam example has relatively lower overall correlation values, the smallest scale is the highest followed by a steady decrease and then also stabilizing at larger scales. Lastly, we can also derive statistical conclusions because, in

the firm condition, the two series are correlated at all scales, whereas the series are only correlated beyond chance at the smaller scales in the foam condition.

Multiscale Regression Analysis. Multiscale regression analysis (MRA) is a further generalization of DCCA that brings the analyses into a predictive, regression framework (Kristoufek, 2015b). The key questions that can be answered by it are: a) *How does the influence of one time series on another time series change as a function of scale?* and b) *What is/are the dominant (time) scale(s) of influence of one time series on another time series?* The algorithm is largely the same as DCCA, with a key difference being that instead of estimating scale-wise symmetric correlation coefficients, leveraging methods of Ordinary Least Squares (OLS) regression, asymmetric β coefficients are estimated (Kristoufek, 2015b; Likens et al., 2019b) according to the following equation:

$$\beta(s) = \frac{F_{xy}(s)}{F_x^2(s)}$$

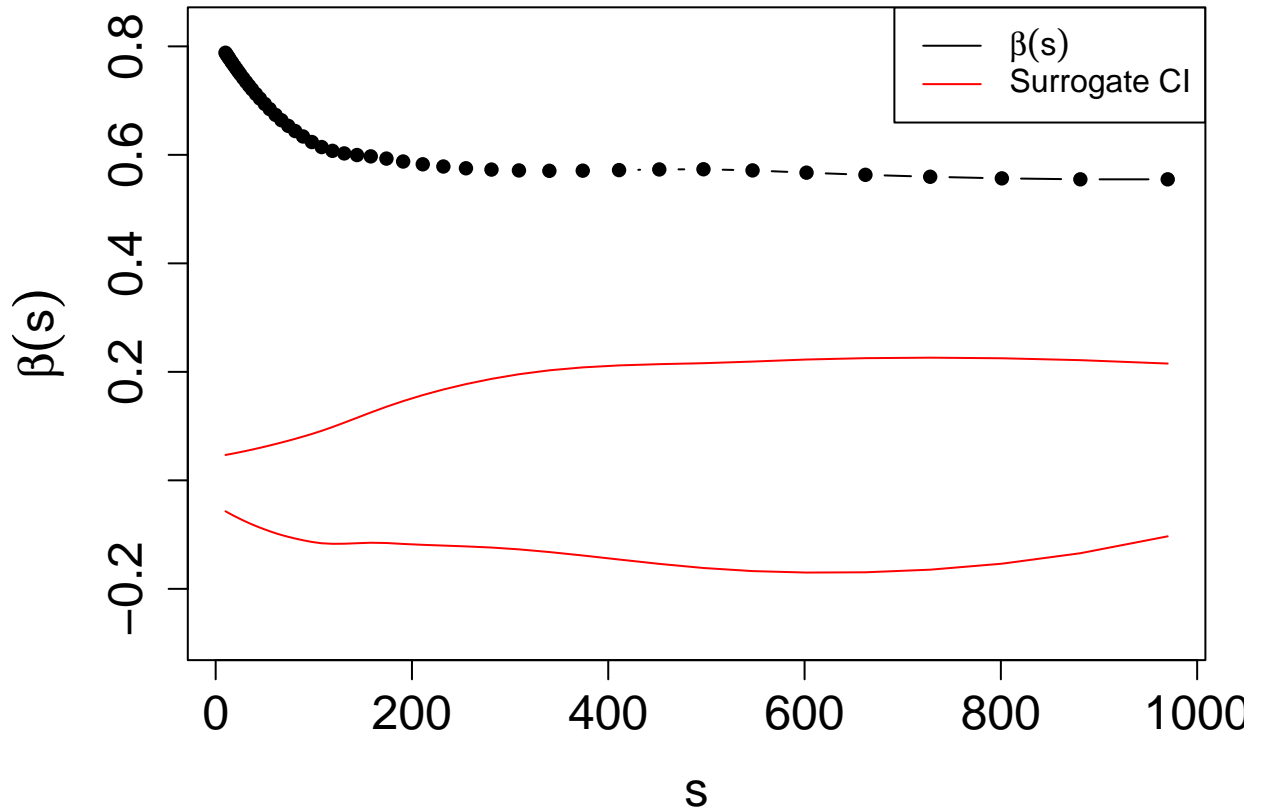
The $\beta(s)$ equation differs from the $\rho(s)$ equation only in the denominator where $F_x^2(s)$ is the average squared residual at each scale and $F_{xy}(s)$ is still the scale-wise covariance.

MRA Examples. Considering the LRC and LRCC simulations used for DCCA, we can examine whether the scale-wise fluctuations of one variable can predict the scale-wise fluctuations of the other using `mra()`. As with a traditional regression approach, we will use one of our variables as our predictor (x_t) and the other as our outcome (y_t). In the example below, we again first define our logarithmically spaced scales. We then apply the `mra()` function to the two simulated time series. In this case, it's important to specify which variable is `x` (the predictor) and which is `y` (the outcome).

```
scales <- logscale(scale_min = 10, scale_max = 1000, scale_ratio = 1.1)

mra.out <- mra(x = sim1[,1], y = sim1[,2], order = 1, scales = scales)
```

We can then visualize these results as shown below in Figure 12. Generally, we observe that the β coefficients are relatively stable at increasing time scales with a general, perhaps quadratically increasing trend. Here it is also important to investigate the change in R^2 as well as the t -values. Below we see that the R^2 is quite high at most of the time scales with $R^2_{min} = 0.67$ and $R^2_{max} = 1.85$ and all $\beta(s)$ exceed the confidence

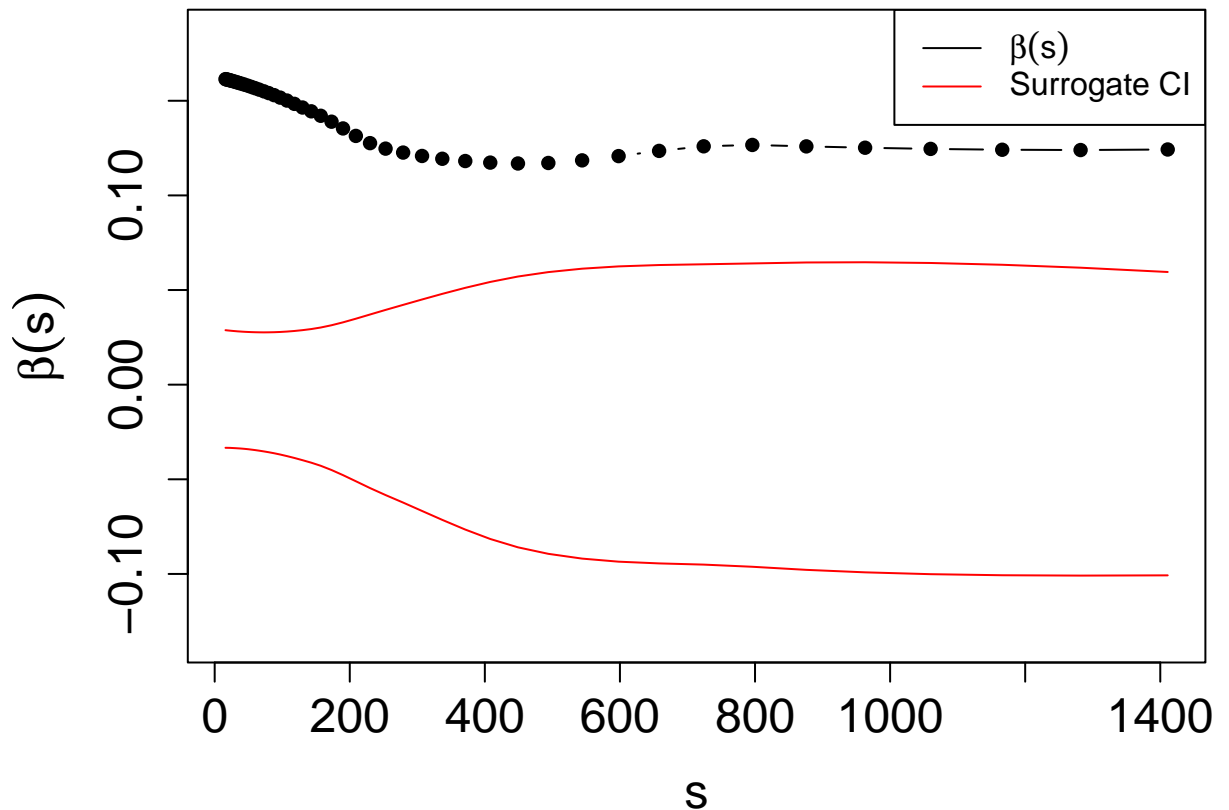


intervals, implying conventional statistical significance. So between these two component ARFIMA processes, the output of MRA shows that much of the scale specific variance in y_t is explained and predicted by x_t .

Figure 12. *MRA output for long range correlation and long range cross-correlation.*

Turning next to the empirical balance data, we can determine whether postural adjustments in the COPx are predictive of adjustments in COPy, and vice versa. This means that we use the `mra()` function two times and reverse the order of entry for the x and y arguments to allow for determining the degree to which each signal can predict the

other across scales. In Figure 13 below, we see the resulting β 's we observed for the the balance data on the firm surface. Notably, the COPx predicting COPy (max $\beta = 0.19$) has noticeably smaller β values compared to COPy predicting COPx (max $\beta = 3.25$). Notice as well how Figure 13 (bottom), where adjustments in the y dimension are predicting adjustments in the x dimension, resembles the DCCA plot for this analysis (see Figure 11). Given the asymmetry in the magnitude of the β s, this example suggests that postural adjustments in the y dimension appear to be driving changes in the x dimension. And, there is a clear time scale where this relationship is strongest at scales = 55, implying a dominant mode of coordination between mediolateral and anteroposterior control processes.



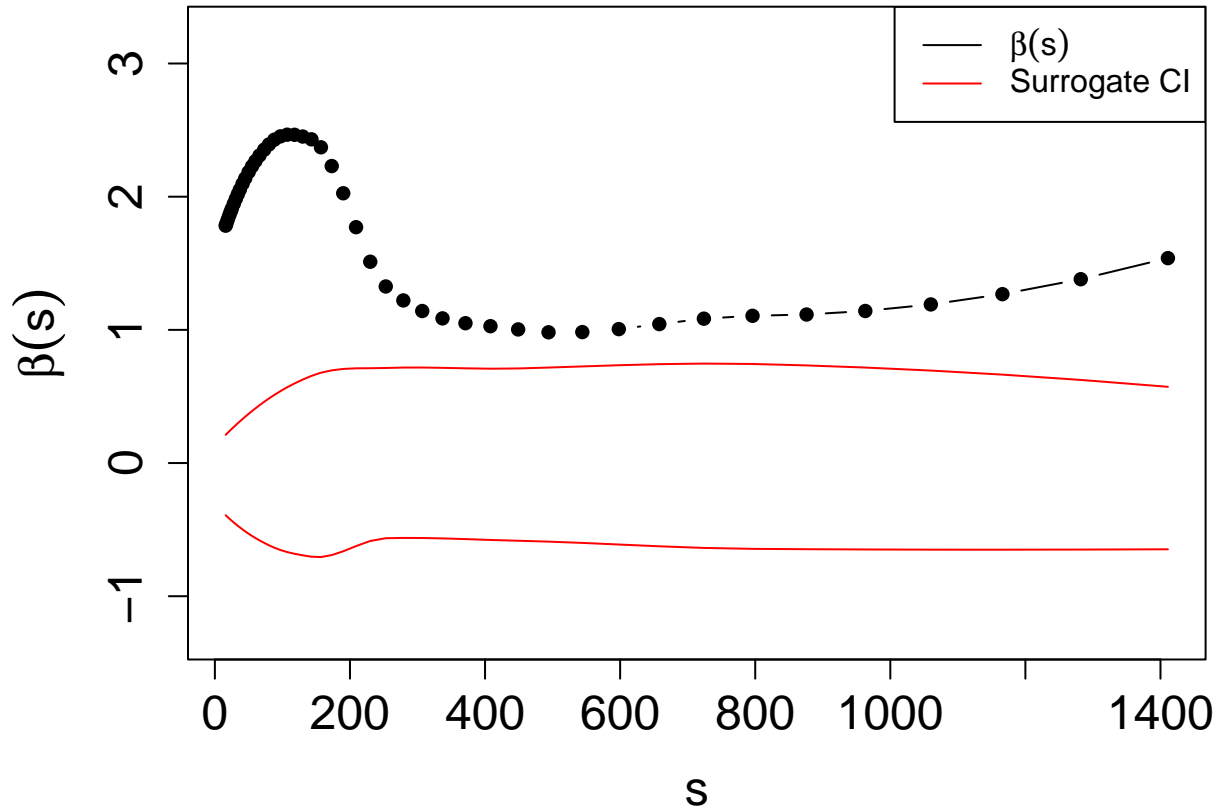


Figure 13. MRA output for balance data on foam surface with COP_x predicting COP_y (top) and COP_y predicting COP_x (bottom).

Surrogate Methods

In all of the above methods, one gets either a single estimate of a parameter (e.g., α) or a range of estimates (e.g., $\rho(s)$, $\beta(s)$). While those estimates are meaningful in and of themselves, it is common practice to perform some form of null hypothesis test regarding the estimate(s). These are generally referred to as surrogate methods (Kantz & Schreiber, 2003). We present several options here that could be ranked in terms of increasing levels of rigor: randomized surrogates, iterative amplitude adjusted Fourier transformed (IAAFT) surrogates, and model-based surrogates.

Randomized Surrogates. Randomized surrogates generally involve randomly shuffling the order of values of a time series. The idea is generally that the temporal structure is destroyed, yet the other features of the time series still exist (Kantelhardt et al., 2002). The confidence intervals for all of our plotting methods use this technique. Note that additional options exist along these lines (see for example (Dumas, Nadel, Soussignan, Martinerie, & Garnero, 2010)). The key comparison here would be to compare the estimates extracted from a given analysis (e.g., DFA) on the observed sample of data with the estimates derived from an equally sized sample of the surrogate series (Kantz & Schreiber, 2003; Moulder, Boker, Ramseyer, & Tschacher, 2018; Wiltshire, Steffensen, & Fiore, 2019).

```
rand.surr <- permute::shuffle(pink.noise)

dfa.rand.surr <- dfa(x = rand.surr, order = 1, verbose = 1,
scale = scales, scale_ratio = 1.1)
```

Randomizing the pink noise time series, which originally exhibited long range correlation ($\alpha = 0.82$), and performing DFA on it, now provides an estimate of $\alpha = 0.55$, which is consistent with a random or white noise process. These values are clearly different, however, performing inferential statistics on a sample of observed estimates compared to surrogate estimates would provide compelling evidence that the temporal dynamics suggested by the observed estimates are different than those derived from a random process.

Iterative Amplitude-Adjusted Fourier Transform Surrogates (IAAFT). The IAAFT algorithm was originally developed as a way to discern whether nonlinearity is a feasible explanation for time series patterns (Schreiber & Schmitz, 1996). More recently, it was proposed as a technique to determine if multifractal indices suggest interaction across scales (Ihlen & Vereijken, 2010). Like with randomized shuffling, estimates derived

from IAAFT surrogates should be also be different from the estimates derived from the empirical time series. Although in this case, the comparison is typically made between the multifractal spectra of the observed time series, and the typical spectrum derived empirically from a set of IAAFT surrogate series.

In the code below, we provide an example for generating IAAFT surrogates using the `iaafft()` function in the package. One enters the `signal`, which is the observed time series, and `N`, the number of surrogates to generate. There are a number of options here, but a common number of surrogates is 19 (Kantz & Schreiber, 2003), which allows one to establish a 95% confidence interval. In practice, surrogates are generated from each observed time series. Here we illustrate the process using only a single time series: the multifractal signal used previously in the MF DFA example. Then we use the same parameters for the `mfdfa()` function, but apply it to all of the IAAFFT surrogates. Note also that surrogate analysis is ‘built-in’ to our plot functions within the package as well with options to return the relevant empirically derived confidence intervals.

```
iaafft.surr <- iaafft(fractaldata$multifractal, N = 19)

iaafft.surr.out <- apply(iaafft.surr, MARGIN = 2, FUN = mfdfa,
q = c(-5:5), order = 1, scales=scales, scale_ratio = 2)
```

Assuming we were using IAAFFT to compare the multifractal width (W) between the observed signal and the surrogate signals, recall that the observed width was $W_{multi} = 1.36$. Now, we can calculate the average multifractal width across all of the generated surrogates and we observe that $W_{surr} = 0.61$, which is narrower than the spectrum from the multifractal signal. In practice, there are many surrogate options (Moulder et al., 2018), but, again, inferential statistics are commonly performed to compare observed estimates to the surrogate estimates to bolster evidence of the inferred dynamics.

Model-based Surrogates. Surrogates can also be generated when a theoretical model exists that explains the data generating process for the observed time series. Well-defined mathematical models of this nature are rare in behavioral sciences, but useful because they allow for more targeted and (potentially) realistic hypothesis testing of the underlying dynamics and how they might change due to experimental constraints. We do not provide a worked out example of such processes, but readers can consult cited papers for examples of this kind (Delignières et al., 2011a; Likens et al., 2019b; Roume et al., 2018).

General Discussion

In this manuscript, we provided details about the first version of a new R package aimed at bringing together a number of fractal methods that we and other researchers have found useful in analyzing a range of behavioral and physiological data. Indeed, these collective methods have found utility in virtually every area of science. Despite that reach, many researchers are still not aware of these methods or lack software for their implementation. This `fractalRegression` package is our effort to bridge those gaps by demonstrating each of several methods first with simulated data, followed by equivalent demonstrations with human movement data (only one of many possible use cases). This allows the reader to see both the ‘best case’ scenario as well as the idiosyncrasies that rear their heads when we transition from the pristine world of simulation to the noisiness inherent in empirical human behavioral data.

Taken together, these methods allow researchers to examine, in univariate time series, the magnitude and direction of long range correlation and/or how that magnitude and direction might change over time. In bivariate cases, these methods allow for determining: (1) how the correlation between time series changes as a function of scale and (2) what the dominant (time) scale(s) of coordination are. Or, relatedly, one can investigate how the influence of one time series on another changes as a function of the scale of observation

while potentially identifying the dominant (time) scale(s) of influence. Thus, these methods provide general value and can answer several types of questions on many types of data. To do so effectively requires careful and appropriate application, though. We next discuss some of these considerations while also referring the reader to other helpful tutorial material.

Practical considerations for univariate methods (DFA, MFDFA). We recommend a few points of consideration in conducting DFA and MFDFA. One is to be sure to evaluate whether there are cross-over points in the log scale-log fluctuation plots (Kantelhardt et al., 2001; Likens et al., 2015; Likens & Stergiou, 2020; Peng et al., 1994; Perakakis, Taylor, Martinez-Nieto, Revithi, & Vila, 2009). Cross-over points (or a visible change in the slope as a function of scale) indicate that a simple mono-fractal characterization does not sufficiently characterize the data. If cross-over points are evident, we recommend proceeding to estimate the two scaling regions with a piece-wise regression (as we showed for the empirical DFA example). Note, however, that for the empirical MFDFA example above, we did not parse the signal for piece-wise MFDFA although some efforts have been conducted for decomposing crossovers in multifractal signals (Nagy, Mukli, Herman, & Eke, 2017). Other suggestions are to only analyze a single linear region (Ihlen, 2012). Regardless, more research is needed to understand the implications of crossover phenomena with respect to the more complicated fluctuation functions of MFDFA.

While it is common to use only linear detrending with DFA, this is not necessarily the best practice. Instead, a more rigorous approach requires inspection of trends in the data to determine if a higher order polynomial would be more appropriate for detrending. There are certainly instances in the literature where DFA fluctuation plots show signs of curvilinearity (Delignières et al., 2011b). Such curvilinearity could be interpreted as representing an inflection point. In such cases, one can compare the DFA output for different polynomial orders (Kantelhardt et al., 2001) to determine if a genuine inflection point is present or if nonlinearity in DFA and MFDFA emerges due to unaddressed

nonlinear trends in the original series (Likens et al., 2019b). Indeed, one is not simply limited to OLS detrending with polynomials. Many other propositions have been introduced to generalize the idea of detrending function to other models such as moving averages (Xu et al., 2005) and even non-parametric techniques like empirical mode decomposition (Qian, Gu, & Zhou, 2011). Those and other more ‘exotic’ detrending techniques will be featured in future releases of this package (see Development Plan below).

Another important matter concerns the length of the time series being analyzed. Unfortunately, all of the methods presented in this manuscript are relatively data hungry. The general trend is that estimation error of various quantities detailed above grows dramatically as time series length decreases (Delignieres et al., 2006). That work and other simulation studies have revealed that reliable estimates of fractal quantities requires a minimum length of the time series of ~512 observations although larger is better (Delignieres et al., 2006; Likens et al., 2019b). That recommendation holds true for both univariate and bivariate cases, alike. If multiple time series are to be compared, then it’s also important that they have matching lengths. Relatedly, general recommendations for choosing the min and max scale are a minimum scale of 10 and a maximum scale of $N/4$, where N is the total number of observations in the signal. See Eke, Herman, Kocsis, and Kozak (2002) and Gulich and Zunino (2014) for additional considerations but also keep in mind specific research areas may also have other criteria (Damouras, Chang, Sejdić, & Chau, 2010; Marmelat & Meidinger, 2019).

Practical considerations for bivariate methods (DCCA, MRA). As suggested above, all of the above considerations also apply in the bivariate case such as recommendations for length, scales sizes, and detrending. This is not surprising given that those methods share a common mathematical girding. However, given that the estimands in DCCA and MRA are qualitatively different that those in DFA and/or MFDA, there are likewise some unique issues as well. Regarding time series length, previous research has shown that $\hat{\beta}(s)$ is unbiased regardless of series length and underlying distribution;

however, it’s variance increases dramatically with decreasing time series length, especially for large time scales (Likens et al., 2019b). This has important consequences for evaluation of statistical significance of $\hat{\beta}(s)$ for large s . Namely, ever larger $\hat{\beta}(s)$ may be needed to exceed conventional levels of significance (e.g., $p < .05$). While $\hat{\beta}(s)$ is unbiased, even for non-Gaussian, time series, that property does not hold in the presence of trends (e.g., linear, quadratic) or nonstationarity. In both those instances, $\hat{\beta}(s)$ becomes positively biased, which could imply spurious positive relationships between series if not addressed. In both those instances, one promising remedy seems to be higher order detrending polynomials (e.g., quadratic, cubic). This remedy also seems to apply, even when the underlying increments of nonstationary processes have non-Gaussian distributions. Therefore, it is of utmost importance to inspect time series for strong time trends (e.g., via OLS regression with various powers of time as a predictors) and nonstationarity (e.g., Dickey-Fuller tests) so that a detrending function of sufficient order can be selected for use in the analysis.

Development Plan. The current release version of the `fractalRegression` package features all of the functions presented in Table 1. Other functions are also currently available for research and development but should be considered “works in progress” as they require additional testing but will be elevated in future releases of the package. For example, lagged versions of DCCA and MRA, known as Detrended Lagged Cross Correlation Analysis (DLCCA) or Multiscale Lagged Regression Analysis (MLRA) respectively, are forthcoming. Those methods pose some new challenges for scientists. For example, choosing an optimal time lag requires careful consideration in this multiscale context. Time lag selection can, in part, be based on theoretically motivated temporal distance in which the two processes are expected to be related. However, new research questions may not carry that level of specificity. In this case, it can also be a process of trial and error to determine the maximum lag to include in the analysis using visual inspection. More rigorously, there are other methods for determining a maximum time lag

using a critical value that is dependent on time scales (Shen, 2015); we expect those techniques might be generalized for MLRA as well. Table 3 below shows our initial plan for functions to include in future iterations of the package. Of course, as the package becomes more utilized, new ideas and resources may be come available to build on the current functionality. To that end, we welcome feature requests and collaborations to grow the package to meet the diverse needs of the scientific community.

Table 3

Overview of development plan for `fractalRegression` package

Conclusion

In this paper, we advance the `fractalRegression` R package as a new tool for behavioral, cognitive, and social scientists from varied backgrounds and provide examples of its use on simulated and empirical data. We hope that in collating these methods, and making them efficient, that they will be more accessible and systematically utilized across disciplines. There are many unanswered questions about these methods and the complex dynamics they characterize. Our hope is that this work inspires future efforts that not only apply these methods, but that also expand on them to further our understanding of the complexities of multiscale interactions in dynamic systems.

Open Practices Statement

All data, software and code are included either in this manuscript or in the accompanying manuscript.

Appendix 1: Fundamental Equations

In this appendix, we provide the corresponding equations given for computation of the methods presented in this manuscript and implemented in our package. There is a

natural progression from DFA to DCCA and MRA (Kristoufek, 2015b; Likens et al., 2019b). That progression is given below, starting with:

DFA

$$F_X = \sqrt{\frac{\sum_{j=1}^{T-s+1} f_X^2(s, j)}{T-s}}$$

where

$$f_X^2(s, j) = \frac{\sum_{k=j}^{j+s-1} (X_k - \hat{X}_{k,j})^2}{s-1}$$

DCCA

$$F_Y = \sqrt{\frac{\sum_{j=1}^{T-s+1} f_Y^2(s, j)}{T-s}}$$

where

$$f_Y^2(s, j) = \frac{\sum_{k=j}^{j+s-1} (Y_k - \hat{Y}_{k,j})^2}{s-1}$$

and the scale-wise covariance is estimated as:

$$f_{XY}^2(s, j) = \frac{\sum_{k=j}^{j+s-1} (X_k - \hat{X}_{k,j})(Y_k - \hat{Y}_{k,j})}{s-1}$$

which forms the basis for the scale-wise correlation coefficient estimated as:

$$\rho(s) = \frac{F_{XY}^2(s)}{F_X(s)F_Y(s)}$$

and for the multi-scale regression coefficients, we replace the denominator in the $\rho(s)$ equation with scale-wise variance of the predictor to estimate the scale-wise regression coefficient from regression Y_t on X_t as:

$$\hat{\beta}(s) = \frac{F_{XY}^2(s)}{F_X^2(s)}$$

and where the variance of $\hat{\beta}(s)$ is:

$$\sigma_{\hat{\beta}(s)}^2 = \frac{1}{T-2} \times \frac{F_Y^2(s)}{F_Y^2(s)}$$

and the scale-wise residual variance, $\hat{F}_u^2(s)$ is estimated by applying the DFA algorithm to all scale-wise residuals, $\hat{u}_t(s)$ as:

$$\hat{u}_t(s) = y_t - x_t \hat{\beta}(s) - \overline{y_t - x_t \hat{\beta}(s)}.$$

MF DFA

The foundational equation for MF DFA is similar to that of DFA, following notation from (Kantelhardt et al., 2002), we have

first a profile function for a given time series, $y(t)$

$$Y(i) = \sum_{k=1}^i [x(k) - \bar{x}] \quad \text{for } i = 1, 2, \dots, N,$$

where $x(i)$ is the original time series, \bar{x} is its mean, and N is the length of the time series.

As in DFA we divide the profile function into N_s non-overlapping windows of length s , and within each window, we fit a polynomial function of order m to remove trends and compute the variance

$$F^2(v, s) = \frac{1}{s} \sum_{i=1}^s Y[(v-1)s + i]^2$$

for each segment, $v, v = 1, 2, \dots, N_s$ and

$$F^2(v, s) = \frac{1}{s} \sum_{i=1}^s \{Y[N - (v - N_s)s + i] - y_v(i)\}^2$$

where $y_v(i)$ is fitting polynomial of order m . Next, we average over all segments to obtain the q th order fluctuation function

$$F_q(s) = \left\{ \frac{1}{2N_s} \sum_{v=1}^{2N_s} [F^2(v, s)]^{q/2} \right\}^{1/q}$$

where q can take any real value. Given that $F_q(s)$ generalizes the DFA fluctuation function, F_X , given above, we are interested in understanding how $F_q(s)$ changes with s which we investigate with log-log regressions of those quantities where we expect

$$F_q(s) \sim s^{h(q)}$$

where $h(q)$ is the generalized Hurst exponent. Other fractal quantities can be computed by transformations of $h(q)$. See (Kantelhardt et al., 2002) for details.

Acknowledgments

Author AL receives support from a National Institutes of Health Center grant (P20GM109090), National Science Foundation grant, National Strategic Research Institute/Department of Defense, and the Nebraska Collaboration Initiative.

References

- Bak, P., Tang, C., & Wiesenfeld, K. (1987). Self-organized criticality: An explanation of the 1/f noise. *Physical Review Letters*, 59(4), 381–384. <https://doi.org/10.1103/PhysRevLett.59.381>
- Bianchi, S. (2020). Fathon: A python package for a fast computation of detrended fluctuation analysis and related algorithms. *Journal of Open Source Software*, 5(45), 1828.
- Cavanaugh, J. T., Kelty-Stephen, D. G., & Stergiou, N. (2017). *Multifractality, Interactivity, and the Adaptive Capacity of the Human Movement System: A Perspective for Advancing the Conceptual Basis of Neurologic Physical Therapy*. Retrieved from <https://www.ingentaconnect.com/content/wk/npt/2017/00000041/00000004/art00007>
- Collins, J. J., & De Luca, C. J. (1993). Open-loop and closed-loop control of posture: A random-walk analysis of center-of-pressure trajectories. *Experimental Brain Research*, 95(2), 308–318. <https://doi.org/10.1007/BF00229788>
- Damouras, S., Chang, M. D., Sejdić, E., & Chau, T. (2010). An empirical examination of detrended fluctuation analysis for gait data. *Gait & Posture*, 31(3), 336–340. <https://doi.org/10.1016/j.gaitpost.2009.12.002>
- Davis, T. J., Brooks, T. R., & Dixon, J. A. (2016). Multi-scale interactions in interpersonal coordination. *Journal of Sport and Health Science*, 5(1), 25–34. <https://doi.org/10.1016/j.jshs.2016.01.015>
- Delignieres, D., Ramdani, S., Lemoine, L., Torre, K., Fortes, M., & Ninot, G. (2006). Fractal analyses for ‘short’ time series: A re-assessment of classical methods. *Journal of Mathematical Psychology*, 50(6), 525–544. <https://doi.org/10.1016/j.jmp.2006.07.004>
- Delignières, D., Almurad, Z. M. H., Roume, C., & Marmelat, V. (2016). Multifractal signatures of complexity matching. *Experimental Brain Research*,

- 234(10), 2773–2785. <https://doi.org/10.1007/s00221-016-4679-4>
- Delignières, D., & Torre, K. (2009). Fractal dynamics of human gait: A reassessment of the 1996 data of Hausdorff et al. *Journal of Applied Physiology*, 106(4), 1272–1279. <https://doi.org/10.1152/japplphysiol.90757.2008>
- Delignières, D., Torre, K., & Bernard, P. L. (2011a). Interest of velocity variability and maximal velocity for characterizing center-of-pressure fluctuations. *Science & Motricité*, (74), 31–37. <https://doi.org/10.1051/sm/2011107>
- Delignières, D., Torre, K., & Bernard, P.-L. (2011b). Transition from Persistent to Anti-Persistent Correlations in Postural Sway Indicates Velocity-Based Control. *PLOS Computational Biology*, 7(2), e1001089. <https://doi.org/10.1371/journal.pcbi.1001089>
- Delignières, D., Torre, K., & Lemoine, L. (2008). Fractal models for event-based and dynamical timers. *Acta Psychologica*, 127(2), 382–397. <https://doi.org/10.1016/j.actpsy.2007.07.007>
- Dumas, G., Nadel, J., Soussignan, R., Martinerie, J., & Garnero, L. (2010). Inter-Brain Synchronization during Social Interaction. *PLOS ONE*, 5(8), e12166. <https://doi.org/10.1371/journal.pone.0012166>
- Eddelbuettel, D., & Francois, R. (2011). Rcpp: Seamless R and C++ Integration. *Journal of Statistical Software*, 40(1), 1–18. <https://doi.org/10.18637/jss.v040.i08>
- Eddelbuettel, D., & Sanderson, C. (2014). RcppArmadillo: Accelerating R with high-performance C++ linear algebra. *Computational Statistics & Data Analysis*, 71, 1054–1063. <https://doi.org/10.1016/j.csda.2013.02.005>
- Eke, A., Herman, P., Kocsis, L., & Kozak, L. R. (2002). Fractal characterization of complexity in temporal physiological signals. *Physiological Measurement*, 23(1), R1–R38. <https://doi.org/10.1088/0967-3334/23/1/201>
- Euler, M. J., Wiltshire, T. J., Niermeyer, M. A., & Butner, J. E. (2016). Working

memory performance inversely predicts spontaneous delta and theta-band
scaling relations. *Brain Research*, 1637, 22–33.

<https://doi.org/10.1016/j.brainres.2016.02.008>

Favela, L. H. (2020). Cognitive science as complexity science. *WIREs Cognitive
Science*, 11(4), e1525. [https://doi.org/https://doi.org/10.1002/wcs.1525](https://doi.org/10.1002/wcs.1525)

Garcia, C. A. (2020). *nonlinearTseries: Nonlinear Time Series Analysis*. Retrieved
from <https://CRAN.R-project.org/package=nonlinearTseries>

Ge, E., & Leung, Y. (2013). Detection of crossover time scales in multifractal
detrended fluctuation analysis. *Journal of Geographical Systems*, 15(2), 115–147.
<https://doi.org/10.1007/s10109-012-0169-9>

Goldberger, A. L., Amaral, L. A. N., Hausdorff, J. M., Ivanov, P. C., Peng, C.-K., &
Stanley, H. E. (2002). Fractal dynamics in physiology: Alterations with disease
and aging. *Proceedings of the National Academy of Sciences*, 99(suppl 1),
2466–2472. <https://doi.org/10.1073/pnas.012579499>

Gulich, D., & Zunino, L. (2014). A criterion for the determination of optimal
scaling ranges in DFA and MF-DFA. *Physica A: Statistical Mechanics and Its
Applications*, 397, 17–30. <https://doi.org/10.1016/j.physa.2013.11.029>

Hardstone, R., Poil, S.-S., Schiavone, G., Jansen, R., Nikulin, V. V., Mansvelder, H.
D., & Linkenkaer-Hansen, K. (2012). Detrended Fluctuation Analysis: A
Scale-Free View on Neuronal Oscillations. *Frontiers in Physiology*, 3.
<https://doi.org/10.3389/fphys.2012.00450>

Hausdorff, J. M., Purdon, P. L., Peng, C. K., Ladin, Z., Wei, J. Y., & Goldberger,
A. L. (1996). Fractal dynamics of human gait: Stability of long-range
correlations in stride interval fluctuations. *Journal of Applied Physiology*, 80(5),
1448–1457. <https://doi.org/10.1152/jappl.1996.80.5.1448>

Ihlen, E. A. F. (2012). Introduction to Multifractal Detrended Fluctuation Analysis
in Matlab. *Frontiers in Physiology*, 3. <https://doi.org/10.3389/fphys.2012.00141>

- Ihlen, E. A. F., & Vereijken, B. (2010). Interaction-dominant dynamics in human cognition: Beyond $1/f$? fluctuation. *Journal of Experimental Psychology: General*, 139(3), 436–463. <https://doi.org/10.1037/a0019098>
- Kantelhardt, J. W., Koscielny-Bunde, E., Rego, H. H. A., Havlin, S., & Bunde, A. (2001). Detecting long-range correlations with detrended fluctuation analysis. *Physica A: Statistical Mechanics and Its Applications*, 295(3), 441–454. [https://doi.org/10.1016/S0378-4371\(01\)00144-3](https://doi.org/10.1016/S0378-4371(01)00144-3)
- Kantelhardt, J. W., Zschiegner, S. A., Koscielny-Bunde, E., Havlin, S., Bunde, A., & Stanley, H. E. (2002). Multifractal detrended fluctuation analysis of nonstationary time series. *Physica A: Statistical Mechanics and Its Applications*, 316(1), 87–114. [https://doi.org/10.1016/S0378-4371\(02\)01383-3](https://doi.org/10.1016/S0378-4371(02)01383-3)
- Kantz, H., & Schreiber, T. (2003). *Nonlinear Time Series Analysis*. Retrieved from [/core/books/nonlinear-time-series-analysis/519783E4E8A2C3DCD4641E42765309C7](https://core/books/nonlinear-time-series-analysis/519783E4E8A2C3DCD4641E42765309C7)
- Kello, C. T., Brown, G. D. A., Ferrer-i-Cancho, R., Holden, J. G., Linkenkaer-Hansen, K., Rhodes, T., & Orden, G. C. V. (2010). Scaling laws in cognitive sciences. *Trends in Cognitive Sciences*, 14(5), 223–232. <https://doi.org/10.1016/j.tics.2010.02.005>
- Kelty-Stephen, D. G. (2017). Threading a multifractal social psychology through within-organism coordination to within-group interactions: A tale of coordination in three acts. *Chaos, Solitons & Fractals*, 104, 363–370. <https://doi.org/10.1016/j.chaos.2017.08.037>
- Kelty-Stephen, D. G., Stirling, L. A., & Lipsitz, L. A. (2016). Multifractal temporal correlations in circle-tracing behaviors are associated with the executive function of rule-switching assessed by the Trail Making Test. *Psychological Assessment*, 28(2), 171–180. <https://doi.org/10.1037/pas0000177>
- Kristoufek, L. (2013). Mixed-correlated ARFIMA processes for power-law

cross-correlations. *Physica A: Statistical Mechanics and Its Applications*,
392(24), 6484–6493. <https://doi.org/10.1016/j.physa.2013.08.041>

Kristoufek, L. (2015a). Detrended fluctuation analysis as a regression framework:
Estimating dependence at different scales. *Physical Review E*, 91(2), 022802.
<https://doi.org/10.1103/PhysRevE.91.022802>

Kristoufek, L. (2015b). Detrended fluctuation analysis as a regression framework:
Estimating dependence at different scales. *Physical Review E*, 91(2), 022802.
<https://doi.org/10.1103/PhysRevE.91.022802>

Laib, M., Golay, J., Telesca, L., & Kanevski, M. (2018). Multifractal analysis of the
time series of daily means of wind speed in complex regions. *Chaos, Solitons &
Fractals*, 109, 118–127. <https://doi.org/10.1016/j.chaos.2018.02.024>

Legrand, P., & V  hel, J. L. (2003). Signal and image processing with FracLab.
Thinking in Patterns: Fractals and Related Phenomena in Nature, 321322.

Likens, A. D., Amazeen, P. G., West, S. G., & Gibbons, C. T. (2019a). Statistical
properties of Multiscale Regression Analysis: Simulation and application to
human postural control. *Physica A: Statistical Mechanics and Its Applications*,
532, 121580. <https://doi.org/10.1016/j.physa.2019.121580>

Likens, A. D., Amazeen, P. G., West, S. G., & Gibbons, C. T. (2019b). Statistical
properties of Multiscale Regression Analysis: Simulation and application to
human postural control. *Physica A: Statistical Mechanics and Its Applications*,
532, 121580. <https://doi.org/10.1016/j.physa.2019.121580>

Likens, A. D., Fine, J. M., Amazeen, E. L., & Amazeen, P. G. (2015). Experimental
control of scaling behavior: What is not fractal? *Experimental Brain Research*,
233(10), 2813–2821. <https://doi.org/10.1007/s00221-015-4351-4>

Likens, A. D., & Stergiou, N. (2020). *A tutorial on fractal analysis of human
movements* (N. Stergiou, Ed.). London, United Kingdom: Elsevier.
<https://doi.org/10.1016/B978-0-12-813372-9.00010-5>

Marmelat, V., & Meidinger, R. L. (2019). Fractal analysis of gait in people with parkinson's disease: Three minutes is not enough. *Gait & Posture*.

<https://doi.org/10.1016/j.gaitpost.2019.02.023>

Moulder, R. G., Boker, S. M., Ramseyer, F., & Tschacher, W. (2018). Determining synchrony between behavioral time series: An application of surrogate data generation for establishing falsifiable null-hypotheses. *Psychological Methods*, 23(4), 757–773. <https://doi.org/10.1037/met0000172>

Nagy, Z., Mukli, P., Herman, P., & Eke, A. (2017). Decomposing multifractal crossovers. *Frontiers in Physiology*, 8. Retrieved from <https://www.frontiersin.org/articles/10.3389/fphys.2017.00533>

Peng, C.-K., Buldyrev, S. V., Havlin, S., Simons, M., Stanley, H. E., & Goldberger, A. L. (1994). Mosaic organization of DNA nucleotides. *Physical Review E*, 49(2), 1685–1689. <https://doi.org/10.1103/PhysRevE.49.1685>

Perakakis, P., Taylor, M., Martinez-Nieto, E., Revithi, I., & Vila, J. (2009). Breathing frequency bias in fractal analysis of heart rate variability. *Biological Psychology*, 82(1), 82–88. <https://doi.org/10.1016/j.biopsycho.2009.06.004>

Podobnik, B., & Stanley, H. E. (2008). Detrended Cross-Correlation Analysis: A New Method for Analyzing Two Nonstationary Time Series. *Physical Review Letters*, 100(8), 084102. <https://doi.org/10.1103/PhysRevLett.100.084102>

Qian, X.-Y., Gu, G.-F., & Zhou, W.-X. (2011). Modified detrended fluctuation analysis based on empirical mode decomposition for the characterization of anti-persistent processes. *Physica A: Statistical Mechanics and Its Applications*, 390(23), 4388–4395. <https://doi.org/10.1016/j.physa.2011.07.008>

Roume, C., Almurad, Z. M. H., Scotti, M., Ezzina, S., Blain, H., & Delignières, D. (2018). Windowed detrended cross-correlation analysis of synchronization processes. *Physica A: Statistical Mechanics and Its Applications*, 503, 1131–1150. <https://doi.org/10.1016/j.physa.2018.08.074>

- 774 Santos, D. A., & Duarte, M. (2016). A public data set of human balance
775 evaluations. *PeerJ*, 4, e2648. <https://doi.org/10.7717/peerj.2648>
- 776 Schaworonkow, N., & Voytek, B. (2021). Longitudinal changes in aperiodic and
777 periodic activity in electrophysiological recordings in the first seven months of
778 life. *Developmental Cognitive Neuroscience*, 47, 100895.
779 <https://doi.org/10.1016/j.dcn.2020.100895>
- 780 Schreiber, T., & Schmitz, A. (1996). Improved surrogate data for nonlinearity tests.
781 *Physical Review Letters*, 77(4), 635–638.
782 <https://doi.org/10.1103/PhysRevLett.77.635>
- 783 Shen, C. (2015). Analysis of detrended time-lagged cross-correlation between two
784 nonstationary time series. *Physics Letters A*, 379(7), 680–687.
785 <https://doi.org/10.1016/j.physleta.2014.12.036>
- 786 Snow, E. L., Likens, A. D., Allen, L. K., & McNamara, D. S. (2016). Taking
787 Control: Stealth Assessment of Deterministic Behaviors Within a Game-Based
788 System. *International Journal of Artificial Intelligence in Education*, 26(4),
789 1011–1032. <https://doi.org/10.1007/s40593-015-0085-5>
- 790 Stephen, D. G., Boncoddio, R. A., Magnuson, J. S., & Dixon, J. A. (2009). The
791 dynamics of insight: Mathematical discovery as a phase transition. *Memory &*
792 *Cognition*, 37(8), 1132–1149. <https://doi.org/10.3758/MC.37.8.1132>
- 793 Team, R. C. (2018). *R: A language and Environment for Statistical Computing*.
794 Vienna, Austria.
- 795 Van Orden, G. C., Holden, J. G., & Turvey, M. T. (2003). Self-organization of
796 cognitive performance. *Journal of Experimental Psychology: General*, 132(3),
797 331–350. <https://doi.org/10.1037/0096-3445.132.3.331>
- 798 Wiltshire, T. J., Steffensen, S. V., & Fiore, S. M. (2019). Multiscale movement
799 coordination dynamics in collaborative team problem solving. *Applied*
800 *Ergonomics*, 79, 143–151. <https://doi.org/10.1016/j.apergo.2018.07.007>

801 Xu, L., Ivanov, P. Ch., Hu, K., Chen, Z., Carbone, A., & Stanley, H. E. (2005).

802 Quantifying signals with power-law correlations: A comparative study of
803 detrended fluctuation analysis and detrended moving average techniques.

804 *Physical Review E*, 71(5), 051101. <https://doi.org/10.1103/PhysRevE.71.051101>

805 Zebende, G. F. (2011). DCCA cross-correlation coefficient: Quantifying level of

806 cross-correlation. *Physica A: Statistical Mechanics and Its Applications*, 390(4),

807 614–618. <https://doi.org/10.1016/j.physa.2010.10.022>

Table 1

Table 1. Overview of core package functions, objectives, and output

| Function | Objective | Output |
|------------------------|---|--|
| <code>dfa()</code> | Estimate long-range correlation in a time series | Object containing the overall α estimate and, if desired the <code>logScales</code> and <code>logRMS</code> |
| <code>mfdfa()</code> | Estimate the magnitude and range of long-range correlations in a time series | Object containing the log scales used for the analysis, the log fluctuation function for each scale and q , the various q -order exponents, Hq , τ , h , and Dh . The base of \log depends on scale construction and user input |
| <code>dcca()</code> | Estimates of scale-specific correlation between two time-series | Object containing the scales used for the analysis and the ρ 'rho' values for each scale |
| <code>mra()</code> | Estimates the scale specific regression coefficients for a predictor time series on and outcome time series | Object containing the scales and scale specific β estimates and R^2 . |
| <code>fgn_sim()</code> | Simulate univariate fractional Gaussian noise | Returns a vector of length <code>N</code> according to the specified <code>H</code> Hurst exponent |

| Function | Objective | Output |
|--------------------------|--|--|
| <code>mBm_mGn()</code> | Simulate univariate multi-fractional Brownian motion and Gaussian noise | Returns two vectors of length N according to the specified H_t series |
| <code>mc_ARFIMA()</code> | Simulate various types of bivariate correlated noise processes. | Returns two vectors of length N according to the specified noise process and parameters |
| <code>iaaft()</code> | Generate surrogate series using the iterative amplitude adjusted Fourier transform | Returns a vector of same length as input time series |

Table 2

Results from piece-wise regression analysis

| | Estimate | SE | <i>t</i> | 95% CI l | 95% CI u |
|---------|----------|------|----------|----------|----------|
| Slope 1 | 1.36 | 0.03 | 40.66 | 1.30 | 0.40 |
| Slope 2 | 0.43 | 0.01 | 31.25 | 1.43 | 0.45 |

Table 3

Table 3. Overview of development plan for `fractalRegression` package

| Function | Next Release | Future Release |
|--|--------------|----------------|
| DLCCA | X | |
| MLRA | X | |
| Chabra-Jensen's Direct Estimation of Multifractal Spectra | X | |
| Wavelet Based Fractal Analyses | | X |
| Multifractal Cross-Correlation Methods | | X |
| Advanced Detrending Methods | | X |
| Bayesian Estimation of Hurst Exponent | | X |
| Time Lag Optimization Function | | X |